

# Computing Optimal Control of Cascading Failure in DC Networks

Qin Ba    Ketan Savla

## Abstract

We consider discrete-time dynamics, for cascading failure in DC networks, whose map is composition of failure rule with control actions. Supply-demand at the nodes is monotonically non-increasing under admissible control. Under the failure rule, a link is removed permanently if its flow exceeds capacity constraints. We consider finite horizon optimal control to steer the network from an arbitrary initial state, defined in terms of active link set and supply-demand at the nodes, to a feasible state, i.e., a state which is invariant under the failure rule. There is no running cost and the reward associated with a feasible terminal state is the associated cumulative supply-demand. We propose two approaches for computing optimal control. The first approach, geared towards tree reducible networks, decomposes the global problem into a system of coupled local problems, which can be solved to optimality in two iterations. When restricted to the class of one-shot control actions, the optimal solutions to the local problems possess a piecewise affine property, which facilitates analytical solution. The second approach computes optimal control by searching over the reachable set, which is shown to admit an equivalent finite representation by aggregation of control actions leading to the same reachable active link set. An algorithmic procedure to construct this representation is provided by leveraging and extending tools for arrangement of hyperplanes and polytopes. Illustrative simulations, including showing the effectiveness of a projection-based approximation algorithm, are also presented.

## I. INTRODUCTION

Cascading failure in physical networks can be modeled via discrete-time dynamics, where the time epochs correspond to component failures. The map of the dynamical system is described in terms of composition of a failure rule with a control policy. A common failure rule is permanent

The authors are with the Sonny Astani Department of Civil and Environmental Engineering at the University of Southern California, Los Angeles, CA. {qba, ksavla}@usc.edu. They were supported in part by NSF CAREER ECCS Project No. 1454729.

removal of a link from the network if its physical flow exceeds capacity. Analysis of such dynamics under a given control policy has attracted considerable attention, primarily through simulations, e.g., see [1]–[5]. However, control *design* is relatively less well understood, e.g., see [6] and our previous work in [7] for few such examples. In this paper, we consider such an optimal control problem for power networks.

The network state is described in terms of active links, i.e., links which have not been removed so far, and the external power injection/withdrawal, also referred to as *supply-demand*, at the nodes. Under the failure rule, at a given network state, links are permanently removed if their power flow exceeds thermal capacity constraint. The control actions correspond to changing supply-demand at the nodes. A network state is called *feasible* if it is invariant under the failure rule, and is called *infeasible* otherwise. We are interested in designing control actions to steer the network from an arbitrary initial state to a terminal feasible state within a given finite time horizon. In this paper, admissible control actions are those under which the magnitude of supply-demand at the nodes is non-increasing, and we consider the setting in which there is no running cost and the cost associated with a terminal feasible state is equal to the negative of cumulative supply-demand associated with that state. We use DC approximation for power flow for tractability, in line with standard practice when multiple power flow computations are involved, e.g., see [6], [8], [9].

The optimal control problem studied in this paper was formulated in [6], [10], where the focus was on low-complexity control policies. To the best of our knowledge, a formal framework for computing optimal control beyond these low-complexity policies is lacking in the literature. The objective of this paper is to develop rigorous approaches to address this shortcoming. This is however a challenging task. The hybrid state space prevents straightforward application of standard optimal control and dynamic programming tools. Furthermore, it is not possible to find a natural ordering in the state space due to non-monotonicity of power flow. Non-monotonicity here refers to counterintuitive behaviors, reminiscent of Braess’s paradox [11], under which removal of links can make an infeasible power network feasible and arbitrary load shedding can make a feasible network infeasible, e.g., see [8], [12]–[14].

We distinguish our work with network interdiction problems, e.g., see [8], [15], [16]. The latter is a static problem to find the smallest set of links whose removal causes a severe blackout. The solutions are based on well-known mixed-integer programming techniques, such as Benders’ decomposition and bilevel programming. On the other hand, we do not allow control of links,

and consider a multistage framework induced by the cascading dynamics. As already mentioned, standard control synthesis methods do not apply straightforwardly to our setting.

We provide two approaches for computing optimal control. The first approach is geared towards tree reducible networks, i.e., networks which can be reduced to a tree by recursively replacing subnetworks between supply-demand nodes with links. For such networks, we decompose the (global) optimal control problem into coupled local problems associated with nodes in the tree corresponding to the reduced network, which can be solved to optimality in two iterations. In the first iteration, from leaves to the root, every node solves the local problem as a function of the local coupling variable, which corresponds to outflow from that node. In the second iteration, in the reverse order from the root to the leaves, the local optimal solutions are instantiated with specific values of the coupling variables. When restricted to control actions which shed load only at  $t = 0$ , the local problems, in spite of non-convexity, possess a piecewise affine property, which facilitates analytical solution.

The second approach computes optimal control by *searching* for an optimal feasible terminal state among the states reachable from the initial condition. This search is made possible by an *equivalent* partition of the one-step reachable set from a network state into a *finite* number of aggregated states, with each corresponding to the same reachable active link set. These partitions are determined by admissibility constraints for control actions (to maintain monotonicity of supply-demand at the nodes), and the link failure rules. Linearity of these constraints allows us to leverage and extend tools from the domain of *arrangement of hyperplanes* e.g., see [17] [18, Chapter 24], and *polytopes*, e.g., see [19] [20], to construct these partitions.

In summary, the paper makes several contributions towards computing optimal control of cascading failure in power networks. First, we cast the problem as multistage optimization involving continuous and discrete variables. While one can use sampling approaches for sub-optimal solution, we provide an exact finite representation through an equivalent finite partition of the one-time reachable set. Second, we provide an algorithmic procedure to construct these partitions by making connections to the problem of arrangement of hyperplanes. This well-studied problem in computational geometry is finding increasing application in engineering domains such as robotics [21], fiber-optic networks [22] and even power networks [9]. Constructing partitions in our case requires a *sweep* operation on polytopes in arbitrary dimensions. A formal approach for this operation, as we provide, is not present in the literature to the best of our knowledge. Third, we provide a decomposition approach to compute optimal control for tree reducible networks in

two iterations. The analytical solution when the control actions are restricted to shedding load only at  $t = 0$  relies on establishing invariance of piece-wise linear property of local optimization problems (when viewed as an operator), which could be of independent interest. In our simulation studies, we also consider optimal solution in certain subspaces, a special case of which is the scaling-based, or proportional, control in [10, Section 6.1.1].

We conclude this section by defining a few notations.  $\mathbf{R}$ ,  $\mathbf{R}_{\geq 0}$  and  $\mathbf{R}_{> 0}$  respectively denote the set of real, non-negative real, and positive real numbers.  $\mathbf{0}$  and  $\mathbf{1}$  denote vectors of all zeros and ones of proper sizes, respectively. For an integer  $n$ ,  $[n] := \{1, 2, \dots, n\}$ .  $|S|$  denotes the cardinality of  $S$ . For a vector  $x \in \mathbf{R}^d$ ,  $\text{diag}(x) \in \mathbf{R}^{d \times d}$  denotes the diagonal matrix whose (diagonal) entries are those of  $x$ . For two vectors  $x$  and  $y$  with the same size,  $x \leq y$  means  $x_i \leq y_i$  for all  $i$ . The same convention is adopted for  $\geq$ ,  $<$  and  $>$ . Given sets  $S_1 \subset \mathbf{R}^n$  and  $S_2 \subset \mathbf{R}^n$ ,  $S_1 + S_2$  denotes the Minkowski sum of  $S_1$  and  $S_2$ . Several technical proofs are postponed until the Appendix.

## II. PROBLEM SETUP

We start by recalling the DC power flow approximation.

### A. DC Power Flow Approximation

In this model, it is assumed that the transmission lines are lossless and the voltage magnitudes are constant at 1.0 unit. The graph topology of the power network is described by an *undirected multigraph*  $\mathcal{G} = (\mathcal{V}, \mathcal{E})$ , that is, multiple parallel links can connect the same two nodes in  $\mathcal{G}$ . For convenience, every link in  $\mathcal{E}$  is arbitrarily assigned a direction – the results in the paper do not depend on the direction convention. Let  $\mathcal{V}_+ \subset \mathcal{V}$  and  $\mathcal{V}_- \subset \mathcal{V}$  be the set of supply and demand nodes respectively<sup>1</sup>. A node is called a *transmission node* if it is neither a supply nor a demand node. Let  $\mathcal{V}_t := \mathcal{V}_+ \cup \mathcal{V}_-$  denote the set of non-transmission nodes. Since the network can loose connectivity under cascading dynamics, we let  $(\mathcal{V}, \mathcal{E}) = (\mathcal{V}^{(1)}, \mathcal{E}^{(1)}) \cup \dots \cup (\mathcal{V}^{(r)}, \mathcal{E}^{(r)})$  denote the partition of the original graph (i.e., the graph at  $t = 0$ ) into its  $r$  connected components. The partition will evolve with the dynamics.

The graph  $\mathcal{G}$  is associated with a node-link incidence matrix  $A \in \mathbf{R}^{\mathcal{V} \times \mathcal{E}}$ , where the  $i$ th column  $A_i \in \mathbf{R}^{\mathcal{V}}$  corresponds to link  $i \in \mathcal{E}$  and has +1 and -1 respectively on the tail and head node

<sup>1</sup>In all the figures, except Figure 3, we color supply nodes with blue, and demand nodes with green. For example, see Figure 1.

of link  $i$ , and 0 on other nodes. The links are associated with a flow vector  $f \in \mathbf{R}^{\mathcal{E}}$ ; The signs of elements of  $f$  are to be interpreted as being consistent with the directional convention chosen for links in  $\mathcal{E}$ . We also associate  $\mathcal{G}$  with a diagonal matrix  $W \in \mathbf{R}^{\mathcal{E} \times \mathcal{E}}$  whose diagonal elements give the negative of susceptances, or weights, of the corresponding links. For brevity,  $w_i$  shall denote the  $i$ -th diagonal element of  $W$ . The nodes are associated with phase angles  $\phi \in \mathbf{R}^{\mathcal{V}}$ , and the supply and demand nodes are associated with a supply-demand vector  $p \in \mathbf{R}^{\mathcal{V}}$ ;  $p_i > 0$  for  $i \in \mathcal{V}_+$  and  $p_i < 0$  for  $i \in \mathcal{V}_-$ .

The quantities defined above are related by Kirchhoff's law and Ohm's law in DC approximation as follows:

$$Af = p \quad f = WA^T\phi \quad (1)$$

In order for (1) to be feasible, the supply-demand vector  $p$  needs to be balanced over  $\mathcal{G}^{(i)}$  for all  $i \in [r]$ , that is,

$$p \in \mathcal{B}_{\mathcal{E}} := \left\{ u \in \mathbf{R}^{\mathcal{V}} \mid \sum_{v \in \mathcal{V}^{(i)}} u_v = 0, i \in [r] \right\} \quad (2)$$

For a given network  $\mathcal{G} = (\mathcal{V}, \mathcal{E})$  with balanced supply and demand  $p$ , there exists a unique flow  $f$  satisfying (1), and it is given by [23]:

$$f = WA^T L^\dagger(\mathcal{E})p =: f(\mathcal{E}, p) \quad (3)$$

where  $L(\mathcal{E}) := AW A^T \in \mathbf{R}^{\mathcal{V} \times \mathcal{V}}$  is the weighted Laplacian matrix of  $\mathcal{G}$  and  $L^\dagger(\mathcal{E})$  is its pseudo-inverse. (3) implies that, for a given  $\mathcal{E}$ ,  $f(\mathcal{E}, p)$  is linear in  $p$ .

### B. Cascading Failure Dynamics

Let  $\mathcal{E}^0$  be the initial link set and let  $p^0$  be the initial supply-demand vector satisfying the balance condition in (2). The corresponding link flow  $f$  is uniquely determined by (1) or (3). We associate with each link  $i \in \mathcal{E}^0$  a thermal capacity  $c_i > 0$ . If the magnitude of flow on a link  $i \in \mathcal{E}^0$  exceeds its thermal capacity, i.e.,  $|f_i| > c_i$ , then link  $i$  fails and is removed from the network irreversibly. This changes the topology of the network, causing flow redistribution, which might lead to more link failures, and so on. Such continuing link failures constitute the *uncontrolled* cascading failure dynamics. Note that we consider a link failure rule which is deterministic and which depends solely on the instantaneous flow. This is to be contrasted with other deterministic outage rules based on moving average of successive flows, or stochastic line outage rules, e.g., see [6], [9].

Our objective in this paper is to stop cascading failure through appropriate control actions. While shedding all load at  $t = 0$  achieves this objective trivially, we desire to take control actions that are optimal in a certain sense. Consider the following description of controlled cascading failure dynamics in discrete-time. Each time epoch corresponds to failure of some links (see Remark 1). The node set remains the same. Let  $(\mathcal{E}^t, p^t)$  be the state of the network at time  $t$ , with  $\mathcal{E}^t \subset 2^{\mathcal{E}^0}$  and  $p^t \in \mathbf{R}^{\mathcal{V}}$  denoting the *active link set* and supply-demand vector at time  $t$ , respectively. We consider load shedding as the control and, for convenience, employ control variable  $u \in \mathbf{R}^{\mathcal{V}}$  to be supply-demand vector after load shedding. The controlled cascading failure dynamics, for  $t = 0, 1, \dots$ , and starting from the initial state  $(\mathcal{E}^0, p^0)$ , is given by:

$$(\mathcal{E}^{t+1}, p^{t+1}) = \mathcal{F}(\mathcal{E}^t, p^t, u^t), \quad u^t \in U(\mathcal{E}^t, p^t) \quad (4)$$

where the component functions are  $\mathcal{F}_{\mathcal{E}}(\mathcal{E}, p, u) \equiv \mathcal{F}_{\mathcal{E}}(\mathcal{E}, u) := \{i \in \mathcal{E} \mid |f_i(\mathcal{E}, u)| \leq c_i\}$  and  $\mathcal{F}_p(\mathcal{E}, p, u) \equiv \mathcal{F}_p(u) := u$ .  $\mathcal{F}_{\mathcal{E}}$  is the set of feasible links in  $\mathcal{E}$  under supply-demand vector  $u$ ; and the control input  $u^t$  at time  $t$  becomes the next state supply-demand vector  $p^{t+1}$ . In order for  $\mathcal{F}_{\mathcal{E}}(\mathcal{E}, u)$  to be well-defined,  $u$  must be balanced with respect to the active link set  $\mathcal{E}$ . This is ensured by the following definition of state-dependent control space  $U(\mathcal{E}, p)$ :

$$U(\mathcal{E}, p) = \text{cube}(p) \cap \mathcal{B}_{\mathcal{E}} \quad (5)$$

where  $\text{cube } p := \{u \in \mathbf{R}^{\mathcal{V}} \mid 0 \leq \text{sign}(p_v)u \leq |p_v| \forall v \in \mathcal{V}\}$ , with  $\text{sign}(x)$  being 1 for  $x \geq 0$  and -1 for  $x < 0$ , characterizes the load shedding requirement.  $U(\mathcal{E}, p)$  includes all *admissible* load shedding controls at state  $(\mathcal{E}, p)$ . In particular, if all the supply and demand nodes are disconnected from each other at state  $(\mathcal{E}, p)$ , then  $\mathcal{B}_{\mathcal{E}} = \{\mathbf{0}\}$ , and in this case  $U(\mathcal{E}, p) = \{\mathbf{0}\}$ .

*Remark 1:*

- 1) (4) is of interest only until the time epoch when the link failures stop, e.g., when the network state becomes *feasible* (defined in Section II-C). For the sake of completeness, one can define subsequent time epochs arbitrarily, e.g., at fixed intervals.
- 2) The number of connected components may increase under (4). When this happens at state  $(\mathcal{E}, p)$ , it is possible that  $p \notin \mathcal{B}_{\mathcal{E}}$ . However, (5) ensures that the control action  $u \in U(\mathcal{E}, P)$ , which is the controlled value of  $p$ , is balanced with respect to  $\mathcal{E}$ . Therefore, the balance condition in (2) is operationally satisfied.
- 3) By adopting the steady state DC model in (4), we implicitly neglect the transient power flow dynamics. This is justified by the fact that the transient dynamics evolve at a considerably

faster time scale in comparison to the initial slow-evolving cascade process observed in practice [10]. Along the same reasoning, the cascading dynamics in (4) can be generalized to other systems whose dynamics evolve fast enough so that assuming the system reaching equilibrium between failure epochs is a reasonable approximation. The control action  $u$  is to be then interpreted as adjusting system parameters to choose equilibrium, e.g., (DC) power flow in our setting.

### C. Problem Formulation

Let

$$\mathcal{S} := \{(\mathcal{E}, p) \mid p \in \mathcal{B}_{\mathcal{E}}, |f_i(\mathcal{E}, p)| \leq c_i, \forall i \in \mathcal{E}\} \quad (6)$$

denote the set of *feasible states*. Set  $\mathcal{S}$  is invariant under the uncontrolled cascading dynamics. Note that  $(\mathcal{E}, \mathbf{0}) \in \mathcal{S}$  for every  $\mathcal{E} \in 2^{\mathcal{E}^0}$ . Since  $\mathcal{E}^t, t \geq 0$ , is non-increasing sequence, and  $\mathcal{E}^0$  is finite, the dynamics converges to a feasible state within  $2^{\mathcal{E}^0}$  time epochs.

Our objective is to choose control actions to steer the network from an arbitrary given initial state  $(\mathcal{E}^0, p^0)$  to a feasible state  $(\mathcal{E}^N, p^N) \in \mathcal{S}$  within a given finite horizon  $N$ , while optimizing a certain performance criterion. The control horizon  $N$  is typically much smaller than  $2^{\mathcal{E}^0}$ . Let a generic sequence of control actions over the control horizon be denoted by  $u := (u^0, \dots, u^{N-1})$ . In this paper, we wish to solve the following optimal control problem:

$$\sup_{u \in \mathcal{D}(\mathcal{E}^0, p^0, N)} s^T p^N \quad (7)$$

where  $s \in \{1, 0, -1\}^{\mathcal{V}}$  is a constant defined as:  $s_v := 1$  for  $v \in \mathcal{V}_+$ ,  $s_v := -1$  for  $v \in \mathcal{V}_-$ , and  $s_v := 0$  otherwise, and the set of feasible control actions is defined as:

$$\begin{aligned} \mathcal{D}(\mathcal{E}^0, p^0, N) := \{ & (u^0, \dots, u^{N-1}) \mid u^t \in U(\mathcal{E}^t, p^t) \text{ for } t = 0, \dots, N-1; \\ & (\mathcal{E}^{N-1}, u^{N-1}) \in \mathcal{S}; (\mathcal{E}^t, p^t)_{t \in [N]} \text{ satisfies (4)} \} \end{aligned} \quad (8)$$

For brevity, we shall not show the dependence of  $\mathcal{D}$  on  $\mathcal{E}^0, p^0$  and  $N$  when clear from the context.

*Remark 2:*

- 1) An arbitrary sequence of *admissible* control actions (cf. (5)) is not necessarily *feasible*. (8) implies that, when checking feasibility of a given  $u$ , in addition to checking admissibility, i.e.,  $u^t \in U(\mathcal{E}^t, p^t)$  for  $t = 0, \dots, N-1$ , one also has to check that the failure stops at  $t = N-1$ .

2) In (7), we use supremum rather than maximum because  $\mathcal{D}$  is not closed in general, as illustrated in Example 1 below. This matter is addressed in Section IV-B and it could be ignored before that. The computational complexity of characterizing  $\mathcal{D}$ , and hence of solving (7) is attributed to the cascading dynamics in (4).

*Example 1:* Consider the optimal control problem in (7) for the network shown in Fig. 1a, for  $N = 3$ . Node 1 is the supply node and nodes 2 and 3 are the demand nodes. The initial supply-demand vector is  $p^0 = [30, -10, -20]^T$ . The link weights are  $w = [2, 1, 1, 1]^T$  and the link capacities are  $c = [6, 7, 14, 5]^T$ . Consider  $u^0 = \alpha_k = [21 + 2/k, -7 - 1/k, -14 - 1/k]^T$  for some  $k \geq 1$ . The resulting flow is  $f(\mathcal{E}^0, u^0) = [8 + 6/(7k), 4 + 3/(7k), 9 + 5/(7k), 5 + 2/(7k)]^T$ . Consequently, links  $e_1$  and  $e_4$  fail due to flow exceeding capacity, and the resulting  $\mathcal{E}^1$  is shown in Fig. 1b. For  $u^1 = \alpha_\infty = [21, -7, -14]^T$ ,  $f_2(\mathcal{E}^1, u^1) = 7 \leq c_2$ ,  $f_3(\mathcal{E}^1, u^1) = 14 \leq c_3$ , and therefore there are no more link failures. This implies that  $u(k) := (\alpha_k, \alpha_\infty, \alpha_\infty) \in \mathcal{D}$  for every  $k \geq 1$ . However,  $\hat{u} = \lim_{k \rightarrow \infty} u(k) = (\alpha_\infty, \alpha_\infty, \alpha_\infty) \notin \mathcal{D}$ . This is because  $f(\mathcal{E}^0, \alpha_\infty)$  is such that only link  $e_1$  fails. The resulting  $\hat{\mathcal{E}}^1$  is shown in Fig. 1c and  $f(\hat{\mathcal{E}}^1, \alpha_\infty) = [\text{null}, 28/3, 35/3, 7/3]^T$ , which implies that  $e_2$  fails. Thereafter,  $\hat{\mathcal{E}}^2 = \{e_3, e_4\}$ ,  $f_3(\hat{\mathcal{E}}^2, \alpha_\infty) = 21 > c_3$  and  $f_4(\hat{\mathcal{E}}^2, \alpha_\infty) = 7 > c_4$ . All links fail under  $\hat{u}$  and thus  $\hat{u} \notin \mathcal{D}$ . This demonstrates that  $\mathcal{D}$  is not closed for the given choice of network parameters.

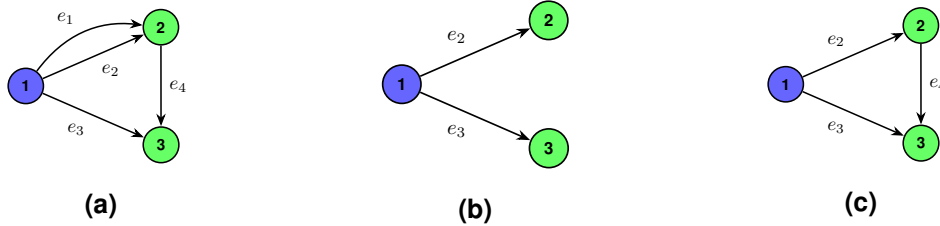


**Fig. 1:** The graph topology for the network used in Example 1 to illustrate that the feasible control action set  $\mathcal{D}$  is not necessarily closed.

*Remark 3:* In writing the optimal control problem in (7), we only consider the terminal cost  $s^T p^N$ , in addition to imposing feasibility condition on the terminal state.  $s^T p^N$  is the remaining cumulative supply and demand once the cascading failure stops, and hence is a natural choice for the objective function in (7). Extension to including running cost is discussed in Remark 15.

#### D. Solution via Search

A generic approach to solving (7) is by performing a *search*, e.g., see [24, Chap 3], on a directed tree composed of the states reachable from the initial state  $(\mathcal{E}^0, p^0)$  in most  $N$  time steps. In other words, the tree is rooted at  $(\mathcal{E}^0, p^0)$ , and has depth  $N$ . Each node of the tree corresponds to a state  $(\mathcal{E}, p)$  which is reachable in one time step from its parent node under a control action which is associated with the incoming arc to that node. When considering one time step reachable set from a given node  $(\mathcal{E}, p)$ , one only considers control actions belonging to  $U(\mathcal{E}, p)$ . The set of goal states for the search is  $\mathcal{S}$  and we associate every feasible state  $(\mathcal{E}, p) \in \mathcal{S}$  with a reward  $s^\top p$  and every infeasible state with a reward  $-\infty$ . The objective is to search for a state in  $\mathcal{S}$  with maximal reward.

Let  $J_t(\mathcal{E}, p)$  be the maximum among utilities of all the states that can be reached in at most  $t$  time steps starting from  $(\mathcal{E}, p)$ . Solving (7) is equivalent to computing  $J_N(\mathcal{E}^0, p^0)$ . This computation can be done as follows:

$$J_1(\mathcal{E}, p) = \max_{u \in U(\mathcal{E}, p)} s^\top u \quad \text{s.t.} \quad |f(\mathcal{E}, u)| \leq c_{\mathcal{E}} \quad (9a)$$

$$J_t(\mathcal{E}, p) = \sup_{u \in U(\mathcal{E}, p)} J_{t-1}(\mathcal{F}_{\mathcal{E}}(\mathcal{E}, u), u), \quad t = 2, \dots, N \quad (9b)$$

where (9a) uses the flow capacity constraint to account for the additional constraint to be satisfied by  $u^{N-1}$ , as commented on in Remark 2. (9a) is a linear program with nonempty feasible set (recall  $(\mathcal{E}, 0) \in \mathcal{S}$  for all  $\mathcal{E}$ ) and commonly referred to as *LP power redispatch*, e.g., see [25]. (9b) uses supremum because  $\mathcal{F}_{\mathcal{E}}(\mathcal{E}, u)$ , and hence  $J_{t-1}(\mathcal{F}_{\mathcal{E}}(\mathcal{E}, u), u)$ , is not continuous w.r.t.  $u$ . It is straightforward to see that  $J_1(\mathcal{E}, p) \leq J_t(\mathcal{E}, p) \leq s^\top p$  for all  $(\mathcal{E}, p)$  and  $t \in [N]$ .

Executing tree search, or equivalently implementing (9), is not directly amenable to a computational procedure, since the number of one-step reachable states from  $(\mathcal{E}, p)$ , or equivalently the set of admissible control actions  $U(\mathcal{E}, p)$ , is a continuum in general. A natural strategy is to discretize  $U(\mathcal{E}, p)$ , at the expense of getting less scalable algorithms and approximate solutions. In this paper, we propose the following two approaches for better computational efficiency:

- (I) (semi-)analytic solution for a certain class of networks, or for optimal solution within a certain class of control policies (Section III); and
- (II) an algorithmic procedure to construct an *equivalent* finite abstraction of the set of admissible control actions, such that computing optimal solution over this finite abstraction gives solution to (7) (Section IV).

### III. ANALYTICAL SOLUTION

In this section, we present (semi-)analytical solution to (7) in some special cases.

#### A. Parallel Networks



**Fig. 2:** (a) a parallel network with two links. (b) the network used in Example 2 to illustrate that the set of feasible one-shot control actions can be neither connected nor closed.

A parallel network  $(\{1, 2\}, \mathcal{E})$  consists of two nodes that are connected by multiple parallel links, e.g., see Figure 2a. We set the convention that the links are directed from node 1 (supply) to node 2 (demand). Since  $p_2 = -p_1$ , following (1), the link flows are given by  $f_i = p_1 w_i / \sum_{j \in \mathcal{E}} w_j$  for all  $i \in \mathcal{E}$ . The following monotonicity result is straightforward.

*Lemma 1:* Consider two arbitrary parallel networks  $(\{1, 2\}, \mathcal{E})$  and  $(\{1, 2\}, \mathcal{E}')$  such that  $\mathcal{E} \subseteq \mathcal{E}'$  and two arbitrary supply-demand vectors  $p = p_1[1 \ -1]^T$  and  $p' = p'_1[1 \ -1]^T$  such that  $0 < p_1 \leq p'_1$ . Then the following are true: (i)  $\mathcal{F}_{\mathcal{E}}(\mathcal{E}, p') \subseteq \mathcal{F}_{\mathcal{E}}(\mathcal{E}, p)$ ; and (ii)  $\mathcal{F}_{\mathcal{E}}(\mathcal{E}, p) \subseteq \mathcal{F}_{\mathcal{E}}(\mathcal{E}', p)$ .

*Remark 4:* For a parallel network  $(\{1, 2\}, \mathcal{E})$  and a natural number  $N \geq 1$ , let  $(u^0, \dots, u^{N-1})$  and  $(\tilde{u}^0, \dots, \tilde{u}^{N-1})$  be two sequences of control actions and  $(\mathcal{E}^1, \dots, \mathcal{E}^N)$  and  $(\tilde{\mathcal{E}}^1, \dots, \tilde{\mathcal{E}}^N)$  be the topology sequences, respectively, under two controls. Lemma 1 implies that if  $u_1^t \geq \tilde{u}_1^t$  for all  $0 \leq t \leq N-1$ , then  $\mathcal{E}^t \subseteq \tilde{\mathcal{E}}^t$  for all  $0 \leq t \leq N-1$ .

For all  $i \in \mathcal{E}$ ,  $f_i/c_i = (p_1/\sum_{k \in \mathcal{E}} w_k) \cdot (w_i/c_i)$ . Noting the common factor  $p_1/\sum_{k \in \mathcal{E}} w_k$  among all links, we label links in the increasing order of  $w_i/c_i$ , i.e.,  $w_i/c_i \leq w_j/c_j$  for  $i \leq j$ ,  $i, j \in \mathcal{E}$ . The chronological order of link failures according to (4) is expected to be aligned with the reverse labeling of the links, and is not affected by different load shedding actions, as implied by the following result.

*Lemma 2:* Consider the cascading dynamics (4) for a parallel network  $(\{1, 2\}, \mathcal{E})$ . If  $f_j(t) \leq c_j$  for some  $j \in \mathcal{E}$  and  $t \in [N]$ , then  $f_i(t) \leq c_i$  for all  $i \leq j$ .

*Proof:* Since  $f_j(t) = p_1(t) \frac{w_j}{\sum_{k \in \mathcal{E}} w_k} \leq c_j$ , then, for  $i < j$ , we have  $f_i(t) = p_1(t) \frac{w_i}{\sum_{k \in \mathcal{E}} w_k} = w_i f_j(t) / w_j \leq w_i c_j / w_j \leq c_i$ . The last inequality is due to  $w_i/c_i \leq w_j/c_j$  for all  $i \leq j$ . ■

*Remark 5:* Lemma 2 implies that for all  $t \in [N]$ , there exists  $j \in \mathcal{E}$  such that  $\mathcal{E}^t = [j]$ . Because  $\mathcal{E}^t$  is non-increasing, at most  $|\mathcal{E}| + 1$  number of distinct network topologies can occur in the cascading dynamics.

The monotonicity properties shown in Lemma 1 and the tight characterization of the reachable set of graph topologies, as implied by Remark 5, allows optimal control synthesis relatively easily. Specifically, we show that a *one-shot control* defined next is optimal within all control policies for parallel networks.

*Definition 1:* For an initial supply-demand vector  $p^0 \in \mathbf{R}^{\mathcal{V}}$ , a  $N$  stage control sequence  $(u^0, \dots, u^{N-1})$  is called *one-shot control* if, for some  $0 \leq t_1 \leq N - 1$ ,  $u^t = p^0$  for all  $t < t_1$ ,  $u^{t_1} \in \text{cube } p^0$ , and  $u^t = u^{t_1}$  for all  $t \geq t_1$ . Moreover, if  $t_1 = 0$ , then it is also called *constant control*.

In order to describe the analytical expression of an optimal one-shot control for a parallel network  $(\{1, 2\}, \mathcal{E})$ , we first introduce a few notations. Let  $R_i := (c_i/w_i) \sum_{j=1}^i w_j$  for all  $i \in \mathcal{E}$ . In general,  $R_i$  is neither decreasing nor increasing with respect to  $i$ . The following remark is straightforward.

*Remark 6:*  $R_i$  is the maximum supply or demand the network can support when only the first  $i$  links are active: for all  $i \in \mathcal{E}$ ,  $([i], p^0) \in \mathcal{S}$  if and only if  $p_1^0 \leq R_i$ .

Let  $o_1 := \max \arg \max_{i \in \mathcal{E}} R_i$ , and let  $o_{j+1} := \max \arg \max_{i > o_j} R_i$  if  $o_j < |\mathcal{E}|$ . Let  $\text{end}$  be the maximum number such that  $o_{\text{end}}$  is defined. It is straightforward to see that  $o_1 < o_2 < \dots < o_{\text{end}} = |\mathcal{E}|$  and  $R_{o_1} > R_{o_2} > \dots > R_{o_{\text{end}}} = R_{|\mathcal{E}|}$ . For a given initial balanced supply-demand vector  $p^0 \in \mathbf{R}^2$ , an optimal control depends on the value of  $N$ . A big  $N$  provides more flexibility for control design. A small  $N$  forces to shed big portion of loads at small time instants to ensure network feasibility. For example, for  $N = 1$ , sufficiently large amount of load needs to be shed at  $t = 0$  to ensure that all links become feasible. Next we define a quantity  $N_j(p^0)$  for every balanced  $p^0 \in \mathbf{R}^2$  and  $j \in [\text{end}]$ , which will be used in the specification of optimal control. Let  $(\mathcal{E}_{\text{un}}^0, \dots, \mathcal{E}_{\text{un}}^N)$  be the non-increasing topology sequence of the uncontrolled cascading dynamics (4) (that is,  $u^t = p^0$  for all  $t$ ). Let  $R_{o_0} := \infty$ ,  $R_{o_{\text{end}+1}} = 0$  and  $\mathcal{E}_{\text{un}}^{-1} \supset \mathcal{E}_{\text{un}}^0$  for convenience. Let  $j \in [\text{end}] \cup \{0\}$  be such that  $R_{o_{j+1}} < p_1^0 \leq R_{o_j}$  and let  $N_k(p^0) := 1 + \min \{t \in \{0, \dots, N\} \mid (\mathcal{E}_{\text{un}}^t, p^0) \in \mathcal{S}\}$  for  $1 \leq k \leq j$  and  $N_k$  be such that  $\mathcal{E}_{\text{un}}^{N_k(p^0)-1} \subseteq [o_k] \subset \mathcal{E}_{\text{un}}^{N_k(p^0)-2}$  for all  $j+1 \leq k \leq \text{end}$ . The above definition implies that  $|\mathcal{E}| \geq N_1(p^0) \geq \dots \geq N_{\text{end}}(p^0) = 1$  for all  $p^0$ . Finally, let  $N_0(p^0) := \infty$  for all  $p^0$  for convenience.

*Proposition 1:* Consider a parallel network  $(\{1, 2\}, \mathcal{E})$  with link weights  $w \in \mathbf{R}_{>0}^{\mathcal{E}}$ , flow

capacities  $c \in \mathbf{R}_{>0}^{\mathcal{E}}$  and initial supply demand vector  $p^0$ . If  $N_j(p^0) \leq N < N_{j-1}(p^0)$ , then an optimal control action is as follows:  $u^{t,*} = p^0$  for all  $0 \leq t < N_j(p^0) - 2$  and  $u^{t,*} = \min\{R_{o_j}, p_1^0\}[1 \ -1]$  for all  $\max\{N_j(p^0) - 2, 0\} \leq t \leq N - 1$ .

*Remark 7:* While Proposition 1 gives the explicit expression for a one-shot control that is optimal for parallel networks, the optimality of one-shot control in more general settings is proven in [12].

*Corollary 1:* For a parallel network  $(\{1, 2\}, \mathcal{E})$  with link weights  $w \in \mathbf{R}_{>0}^{\mathcal{E}}$ , flow capacities  $c \in \mathbf{R}_{>0}^{\mathcal{E}}$  and initial supply demand vector  $p^0$ , for  $N \geq |\mathcal{E}| - o_1$ , the following constant control  $u^*$  is an optimal control:  $u^{t,*} = [1 \ -1] \min\{p_1^0, R_{o_1}\}$  for all  $0 \leq t \leq N - 1$ .

On one hand, Proposition 1 and Corollary 1 justify the study of optimal control within a special class of control policies. On the other hand, while a one-shot control action can be optimal for non-parallel networks, it is not true in general. Furthermore, the sets of feasible constant and one-shot control actions are not necessarily closed nor connected. These are illustrated in the following example.

*Example 2:* Consider the network illustrated in Fig. 2b, containing a single supply node 1 and a single demand node 3, having link weights  $w = \mathbf{1}$ , and with initial supply-demand vector  $p^0 = [3, 0, -3]^T$ . Consider two scenarios corresponding to link capacities  $c^1 = [0.8, 1.5, 0.6, 0.5, 0.25]^T$  and  $c^2 = [0.8, 1.5, 0.7, 0.5, 0.25]^T$ , where note that the two scenarios differ only in the capacity of link  $e_3$ . We consider the optimal control problem for  $N = 2$ . Let  $u^t = z_t \times [1, 0, -1]^T$ ,  $t \in \{0, 1\}$ ,  $0 \leq z_1 \leq z_0$  be the control actions. The flow under  $u^t$  for relevant network topologies are:  $f(\{5\}, u^t) = \frac{1}{4}z_t \times [1, 2, 1, 1, 1]^T$ ,  $f(\{4\}, u^t) = \frac{1}{5}z_t \times [1, 3, 2, 1]^T$ ,  $f(\{3\}, u^t) = \frac{1}{3}z_t \times [1, 2, 1]^T$  and  $f(\{2\}, u^t) = z^t$ . The maximal value of  $z_t$  can be supported by these networks are, respectively, 1, 1.5, 1.8, 1.5 in the first scenario and 1, 1.75, 2.1, 1.5 in the second scenario. It is straightforward to see that the network would get disconnected in both scenarios if no load shedding is implemented. By considering all possible topology sequences that can occur under a control policy, we obtain the following:

- (i) The best one-shot control that sheds loads at  $t = 1$  is  $z_0 = 3$ ,  $z_1 = 1.5$  in both scenarios.
- (ii) The best constant controls are:  $z_0 = z_1 = 1.5$  in the first scenario and  $z_0 = z_1 = 2.1$  in the second scenario.
- (iii) An optimal control is  $z_0^* = 2.1$  and  $z_1^* = 1.8$  in the first scenario and is  $z_0^* = z_1^* = 2.1$  in the second scenario.

We can see that in both cases, the best constant controls perform no worse than the best one-shot controls, and while the best constant control is not optimal over all controls in the first scenario, it is optimal in the second scenario. Furthermore, in the second scenario, the set of feasible constant controls is  $\{(x, x) \mid x \in [0, 1] \cap (2, 2.1]\}$  and is neither connected nor closed.

### B. A Decomposition Approach for Tree Reducible Networks

In this section, we develop a decomposition approach to compute optimal control for *tree reducible networks*.

*Definition 2 (Tree Reducible Network):* A network  $\mathcal{G} = (\mathcal{V}, \mathcal{E})$  with supply-demand vector  $p$  is called tree reducible if it is a tree, or it can be reduced to a tree<sup>2</sup>  $\mathcal{T} = (\mathcal{V}_T, \mathcal{E}_T)$  by recursively replacing subnetworks, which is between two nodes and contains no supply or demand nodes in the interior, with single links. In this case, the subnetworks and  $\mathcal{T}$  are called, respectively, the reducible components and reduced tree of  $\mathcal{G}$ .

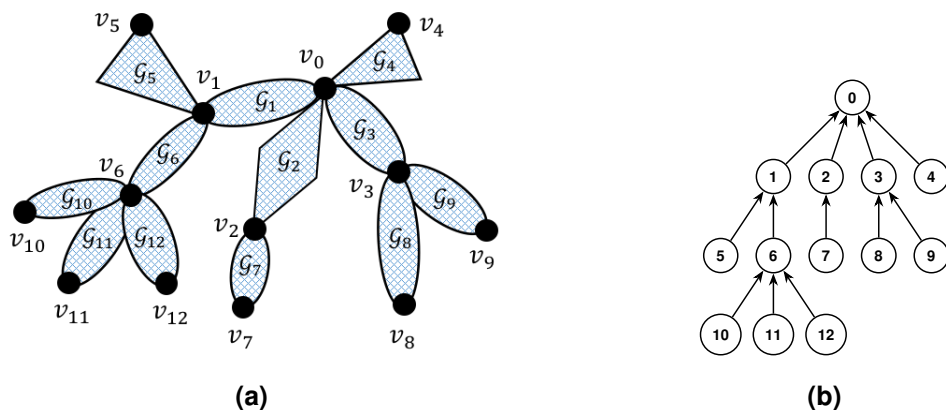


**Fig. 3:** (a) a tree reducible network  $\mathcal{G}$ , which is the residual IEEE 39 bus network in Fig. 9a resulting from removal of links  $e_6, e_{16}$  and  $e_{40}$ , e.g., caused by initial failure. It is assumed that all the nontransmission nodes in the IEEE 39 network are included in relabeled nodes  $v_0, \dots, v_{12}$ , e.g.,  $v_0$  corresponds to node 16 in Fig. 9a; (b) the reduced tree  $\mathcal{T}$  of  $\mathcal{G}$ .

Fig. 3 provides an example of a tree reducible network, which is obtained from IEEE 39 bus network in Fig. 9a. Each sub-network (denoted by  $\mathcal{G}_1, \dots, \mathcal{G}_{12}$ ) in Fig. 3a represents a *reducible component* and corresponds to a link in the *reduced tree*  $\mathcal{T} = (\mathcal{V}_T, \mathcal{E}_T)$  shown in Fig. 3b. We

<sup>2</sup>A tree is an undirected graph in which any two nodes are connected by at most one path.

assign directions for the links in  $\mathcal{E}_T$  as follows<sup>3</sup>. Pick an arbitrary node in  $\mathcal{V}_T$ , and call it the root node. The directions for all the links incident to the root node are chosen to be incoming to the root node. The directions for the remaining links are similarly chosen to be directed towards the root node; see Figure 3b for an example. For the resulting directed tree, we fix a reverse topological ordering<sup>4</sup> of the nodes  $(0, 1, \dots, |\mathcal{V}_T| - 1)$ , with 0 being the root node. Figure 3b illustrates such an ordering. In order to minimize notations, we use the same label for a link and its tail node. For example, the link  $(5, 1)$  in Figure 3b is labeled as link 5. An in-neighbor (resp., out-neighbor) of a given node is called its child (resp., parent) node. For node  $i \in \mathcal{V}_T$ , let  $\mathcal{C}_i$  denote the set of its children nodes, and let  $\bar{\mathcal{C}}_i$  denote the set of nodes consisting of the descendants of  $i$  and the node  $i$  itself. For example, in Fig. 3b,  $\mathcal{C}_1 = \{5, 6\}$  and  $\bar{\mathcal{C}}_1 = \{1, 5, 6, 10, 11, 12\}$ . With this definition,  $\mathcal{V}_T \equiv \bar{\mathcal{C}}_0$ . Node  $i$  is called a *leaf* if it has no child node, i.e., if  $\mathcal{C}_i = \emptyset$ .

Let us start with the simple case when the entire network consists of a single reducible component, say  $\mathcal{G}_i$ , so that the reduced tree is  $\mathcal{T} = (\{v_0, v_1\}, 1)$ , where  $v_0$  and  $v_1$  are the only supply-demand nodes in  $\mathcal{G}_i$ . Let  $a_i \in \{1, 0, -1\}^{\mathcal{V}_i}$  be such that  $a_{i,v}$  is equal to 1 if  $v = v_0$ , is equal to  $-1$  if  $v = v_1$ , and is equal to zero otherwise. We do not fix the individual identities of  $v_0$  and  $v_1$  as supply or demand nodes, and the choice of the signs of entries of  $a_i$  is merely to set some convention. We let  $z_i^t a_i$  with  $z_i^t \in \mathbf{R}$  denote the supply-demand vector in  $\mathcal{G}_i$  for  $t \in [N]$ , or equivalently, the control sequence for  $t \in \{0, \dots, N-1\}$ . If  $\tilde{p}_i a_i$ , for  $\tilde{p}_i \in \mathbf{R}$ , is the initial supply demand vector, then the set of feasible control sequences as per (8) is  $\mathcal{D}(\mathcal{E}_i^0, \tilde{p}_i a_i, N)$ , where  $\mathcal{E}_i^0$  is the initial active link set in  $\mathcal{G}_i$  at  $t = 0$ . Recall that  $\mathcal{D}(\mathcal{E}_i^0, \tilde{p}_i a_i, N)$  captures the constraint that the terminal state at  $t = N$  is feasible, as well as the monotonicity constraint implied by (5). We split these two constraints as  $\mathcal{D}(\mathcal{E}_i^0, \tilde{p}_i a_i, N) = \tilde{\mathcal{D}}_i(N) \cap \hat{\mathcal{D}}_i(N)$ , where  $\tilde{\mathcal{D}}_i(N)$  captures feasibility of terminal state, while relaxing monotonicity, and  $\hat{\mathcal{D}}_i(N)$  captures monotonicity while relaxing

<sup>3</sup>The results presented in the current Section III do not depend on the particular choice of directions for links in  $\mathcal{E}_T$ , as selected here (see also Remark 9).

<sup>4</sup>That is, for every directed link  $(i, j)$ , we have  $i > j$ .

feasibility of the terminal state. These two sets are formally defined as:

$$\begin{aligned} \tilde{\mathcal{D}}_i(N) &:= \{(z_i^0, \dots, z_i^{N-1}) \in \mathbf{R}^N \mid (\mathcal{E}_i^{N-1}, z_i^{N-1} a_i) \in \mathcal{S}; \\ &\quad \mathcal{E}_i^t = \mathcal{F}_{\mathcal{E}}(\mathcal{E}_i^{t-1}, z_i^{t-1} a_i), \forall t \in [N-1]\} \end{aligned} \quad (10)$$

$$\hat{\mathcal{D}}_i(N) := \{(z_i^0, \dots, z_i^{N-1}) \in \mathbf{R}^N \mid z_i^0 \in \text{cube } \tilde{p}_i, z_i^t \in \text{cube } z_i^{t-1}, \forall t \in [N-1]\} \quad (11)$$

When clear from the context, we shall not show the explicit dependence of  $\tilde{\mathcal{D}}_i$  and  $\hat{\mathcal{D}}_i$  on  $N$ .

*Remark 8:*

- 1) Note that  $\tilde{\mathcal{D}}_i$  includes control actions that cause loss of connectivity in  $\mathcal{G}_i$ . In this case, since we have only one supply and demand, the constraint that the terminal state  $(\mathcal{E}_i^{N-1}, z_i^{N-1} a_i)$  is feasible, implies that  $z_i^{N-1} = 0$ . In addition, since all links have symmetrical capacities,  $\tilde{\mathcal{D}}_i = -\hat{\mathcal{D}}_i$ .
- 2)  $\hat{\mathcal{D}}_i$  is a polytope. However,  $\tilde{\mathcal{D}}_i$  is non-convex in general, as indicated by the disconnected feasible set of constant control actions in Example 2. The explicit computation of  $\tilde{\mathcal{D}}_i$  follows from the discussion in Section IV-C (cf. Remark 17).

The flexibility afforded by splitting the control constraints into (10) and (11) for an isolated reducible component allows to translate capacity constraints from individual links in a general tree reducible network  $\mathcal{G}$  into equivalent constraints for the equivalent links in  $\mathcal{E}_T$  as follows. The control  $u_i^t$ <sup>5</sup> at node  $i \in \mathcal{V}_T$  at time  $t \in \{0, \dots, N-1\}$  is split as  $u_i^t = z_i^t - \sum_{j \in \mathcal{C}_i} z_j^t$ . For example, referring to Figure 3,  $u_3^t = z_3^t - z_8^t - z_9^t$ . In this case, the flow on link  $i$  in  $\mathcal{E}_T$ ,  $z_i^t$ , is interpreted as  $\mathcal{G}_i$ 's *share* of control input  $u_i^t$ .  $u_i := (u_i^0, \dots, u_i^{N-1})$ ,  $i \in \mathcal{V}_T$ , is constrained to satisfy (11) for  $\tilde{p}_i = p_i^0$ , and  $z_i := (z_i^0, \dots, z_i^{N-1})$ ,  $i \in \mathcal{E}_T$ , is constrained to satisfy (10). It is clear that, for root node,  $z_0 = \mathbf{0}$ . Hence, let  $\tilde{\mathcal{D}}_0 = \{\mathbf{0}\}$  for convenience.

Consider the following optimization problem that will inform the decomposition approach. For  $i \in \mathcal{E}_T$ , given  $z_i \in \tilde{\mathcal{D}}_i$ , let:  $g_i(z_i) :=$

$$\begin{aligned} &\sup_{\substack{z_k \in \tilde{\mathcal{D}}_k \forall k \in \bar{\mathcal{C}}_i \setminus i \\ u_k \in \hat{\mathcal{D}}_k \forall k \in \bar{\mathcal{C}}_i}} \sum_{k \in \bar{\mathcal{C}}_i} s_k u_k^{N-1} \\ &\text{s.t.} \quad z_k = u_k + \sum_{j \in \mathcal{C}_k} z_j, \quad \forall k \in \bar{\mathcal{C}}_i \end{aligned} \quad (12)$$

(12) can be interpreted as maximizing a certain *utility function* over the subtree rooted at node  $i \in \mathcal{V}_T$ , given that the outflow sequence from node  $i$  is  $z_i \in \mathbf{R}^N$ . (12) is a generalization of (7), in the sense that  $g_0(\mathbf{0})$  is equal to the optimal value of (7). Since the objective function of (12)

<sup>5</sup>With a slight abuse of notation, we use  $u$  to denote control inputs for the original network as well as the reduced network.

is linear and separable and the decision variables are coupled with only equality constraints of a simple form, standard distributed algorithms, for example, ADMM [26], can be used to solve (12) if the sets  $\tilde{\mathcal{D}}_k$  are convex. However,  $\tilde{\mathcal{D}}_k$  are non-convex in general (cf. Remark 8). In order to reduce the complexity due to this non-convexity, we decompose (12) into the following *nested form*:

$$g_i(z_i) = \sup_{\substack{z_j \in \mathcal{Z}_j \forall j \in \mathcal{C}_i \\ u_i \in \tilde{\mathcal{D}}_i}} s_i u_i^{N-1} + \sum_{j \in \mathcal{C}_i} g_j(z_j) \quad (13)$$

s.t.  $z_i = u_i + \sum_{j \in \mathcal{C}_i} z_j$

where  $\mathcal{Z}_j := \tilde{\mathcal{D}}_j \cap \left( \hat{\mathcal{D}}_j + \sum_{k \in \mathcal{C}_j} \mathcal{Z}_k \right)$  combines both the constraints  $z_j \in \tilde{\mathcal{D}}_j$  and  $z_j = u_j + \sum_{k \in \mathcal{C}_j} z_k$ , for all  $j \in \mathcal{E}_T$ . The equivalence between (12) and (13) can be seen via induction. In particular, if  $i$  is a leaf node, then  $\mathcal{C}_i = \emptyset$ . Both (12) and (13) reduce to  $g_i(z_i) = \max_{z_i = u_i \in \hat{\mathcal{D}}_i} s_i u_i^{N-1}$ . The optimal value function is  $g_i(z_i) = s_i z_i^{N-1}$  if  $z_i \in \tilde{\mathcal{D}}_i \cap \hat{\mathcal{D}}_i = \mathcal{Z}_i$ , and is  $-\infty$  otherwise due to infeasibility. If  $i$  is not a leaf node, then (13) can be interpreted as being associated with a local *star* subnetwork in  $\mathcal{T}$ .

The solution to (12) is obtained by solving sub-problems in (13) over two iterations:

- (I) Compute  $g_i : \mathcal{Z}_i \rightarrow \mathbf{R}$  via (13) for every  $i \in \mathcal{V}_T$  in the reverse topological order;
- (II) Set  $z_0^* = \mathbf{0}$ . Following the topological order, for every  $i \in \mathcal{V}_T$ , compute an optimal solution  $(u_i^*, \{z_j^*, j \in \mathcal{C}_i\})$  to (13) corresponding to  $g_i(z_i^*)$ .

It is easy to check that, for all  $i \in \mathcal{V}_T$ , we have  $\mathbf{0} \in \hat{\mathcal{D}}_i$  and  $\mathbf{0} \in \tilde{\mathcal{D}}_i$ , and hence  $\mathbf{0} \in \mathcal{Z}_i$ . Therefore, iteration (II) is well-posed.

*Remark 9:* The optimal solution to (7) as computed by the decomposition approach is invariant with respect to the choice of root node, directions of the links in  $\mathcal{E}_T$ , and the topological ordering used for labeling nodes in  $\mathcal{V}_T$ .

While the decomposition approach reduces complexity of solving (7) for general tree reducible networks, the bottleneck is still non-convexity of the local problems in (13). In Section III-C, we show that, for one-shot controls, the two iterations involving solutions to the local problems in (13) admit closed-form expressions.

### C. Optimal One-shot Control for Tree Reducible Networks

The next result follows straightforwardly from Definition 1. For a general network, it shows how to reduce the problem of finding an optimal one-shot control to that of finding an optimal constant control.

*Lemma 3:* Consider the optimal control problem in (7), restricted to one-shot control actions, over  $N$  stages with initial state  $(\mathcal{E}_{\text{un}}^0, p^0)$ . Let  $(\mathcal{E}_{\text{un}}^0, \dots, \mathcal{E}_{\text{un}}^n)$ ,  $n \leq N - 1$ , be the longest topology sequence of the uncontrolled cascading dynamics (4) such that  $p^0 \in \mathcal{B}_{\mathcal{E}_{\text{un}}^t}$  for  $0 \leq t \leq n$ <sup>6</sup>. Let  $\bar{u}(\mathcal{E}_{\text{un}}^t, N - t)$  be an optimal solution to (7), restricted to constant control actions, over  $N - t$  stages with initial state  $(\mathcal{E}_{\text{un}}^t, p^0)$ . Then, the one-shot control which sheds load to  $\bar{u}^0(\mathcal{E}_{\text{un}}^{t^*}, N - t^*)$  at stage  $t^* \in \operatorname{argmax}_{0 \leq t \leq n} s^T \bar{u}^0(\mathcal{E}_{\text{un}}^t, N - t)$  is optimal.

Following Lemma 3, it is sufficient to focus on constant controls. In this case, the original problem (12) and the sub-problem (13) are simplified to a great extent: for all  $i \in \mathcal{V}_T$ , the decision variables  $z_i$  and  $u_i$  reduce to one dimensional real numbers; the set  $\hat{\mathcal{D}}_i$  reduces to  $\text{cube } p_i^0$  and the set  $\tilde{\mathcal{D}}_i$  reduces to, in general, the union of multiple disjoint intervals. While Remark 17 explains how to compute  $\tilde{\mathcal{D}}_i$  in this case, we make the following remarks.

*Remark 10:*

- 1) For  $N = 1$ , it is straightforward to see that  $\tilde{\mathcal{D}}_i$  is always a single piece of closed interval. For  $2 \leq N \leq 6$ , we computed  $\tilde{\mathcal{D}}_i$  for constant control corresponding to all the node pairs in the IEEE 39 bus network, and found that they were disconnected in less than 5% of the cases. Based on this, we believe the same pattern to hold true also for larger  $N$  as well as other benchmark networks. In fact, we had to choose the parameters very carefully in Example 2 to show disconnectedness of  $\tilde{\mathcal{D}}_i$  under constant control.
- 2) Even in the case of constant controls,  $\tilde{\mathcal{D}}_i$  can be half open (see Example 2) and hence (12) may not admit a solution. Nevertheless, because the objective function in (12) is linear and hence continuous, we use the closure of  $\tilde{\mathcal{D}}_i$  in (12) and hence closure of  $\mathcal{Z}_i$  in (13) for simplicity. Proposition 4 shows, for a more general setting, how to obtain an interior feasible point that is arbitrarily close to the solution of the problem over the closure.

We consider the following generalized problem of (13) for the case of constant controls. In particular, we will provide results on the solution structure of (14) below which enable closed form computation for every recursive step in the two iteration algorithm proposed in Section III-B, as far as constant controls are considered.

$$\begin{aligned}
 g^{\text{out}}(z) &= \Omega\{(g_j^{\text{in}}, X_j)\}_{j \in [n]} := \max_{x \in \mathbf{R}^n} \sum_{j=1}^n g_j^{\text{in}}(x_j) \\
 \text{s.t.} \quad & \mathbf{1}^T x = z; \quad x_j \in X_j, \quad \forall j \in [n]
 \end{aligned} \tag{14}$$

<sup>6</sup>A sufficient, but not necessary, condition for  $p^0 \notin \mathcal{B}_{\mathcal{E}_{\text{un}}^t}$  at some  $t$  is that some non-transmission node becomes isolated at  $t$ .

where  $X_j \subset \mathbf{R}$  is the union of a finite number of disjoint closed intervals for all  $j \in [n]$ . Operator  $\Omega$  maps from  $n$  input functions  $g_j^{\text{in}}$  with restricted domain  $X_j$  to a single output function  $g^{\text{out}}$  with domain  $\sum_{j=1}^n X_j$ , where the domain of  $g^{\text{out}}$  is not explicitly written in (14). Due to the possible disconnected feasible set  $X_j$ , (14) is in general non-convex.

*Remark 11:* (14) becomes (13) with the following substitutions:  $i = 1$ ,  $\mathcal{C}_i = [n] \setminus \{1\}$ ,  $g_1^{\text{in}}(x_1) = s_i x_1$ ,  $X_1 = \text{cube } p_i^0$ ,  $g_j^{\text{in}}(x_j) = g_j(x_j)$  and  $X_j = \mathcal{Z}_j$  for all  $j \in [n] \setminus \{1\}$ .

The class of input functions considered depends on the following construct. For a given point  $\tau = (\tau_1, \tau_2) \in \mathbf{R}^2$ , define a (continuous) piecewise affine function:  $\chi_\tau : \mathbf{R} \rightarrow \mathbf{R}$  as:

$$\chi_\tau(x) := \begin{cases} x - \tau_1 + \tau_2 & x \leq \tau_1 \\ -x + \tau_1 + \tau_2 & x > \tau_1 \end{cases} \quad (15)$$

As shown in Fig 4, function  $\chi_\tau$  contains two rays joining at  $\tau$ , referred to as the *top point* of  $\chi_\tau$ , and intersects the vertical axis at  $(0, \tau_2 - |\tau_1|)$ .

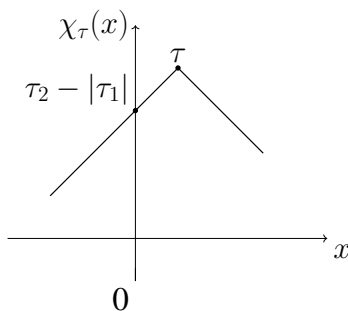


**Fig. 4:** Illustration of  $\chi_\tau(x)$  defined in (15).

It will be useful to consider a  $\chi$  function defined over a restricted domain. When the restricted domain is a closed interval, Lemma 4 can be used to translate the top point into the domain, if not already inside, without changing function values. It is straightforward that, with bounded domain,  $\chi$  functions include linear functions as special cases.

*Lemma 4:* Consider a point  $\tau = (\tau_1, \tau_2) \in \mathbf{R}^2$  and a closed interval  $[b_1, b_2] \subset \mathbf{R}$  such that  $\tau_1 \notin [b_1, b_2]$ , let  $\tau' := (b_2, b_2 - \tau_1 + \tau_2)$  if  $\tau_1 > b_2$  and  $\tau' := (b_1, -b_1 + \tau_1 + \tau_2)$  if  $\tau_1 < b_1$ . Then  $\chi_\tau(x) = \chi_{\tau'}(x)$  for all  $x \in [b_1, b_2]$ .

We first consider the case when  $X_j$  is a single piece of closed interval for all  $j \in [n]$ . As we note in Remarks 10 and 11, we believe that this case is common in practice. In this case, the feasible set of (14) is convex and hence (14) is convex if input functions  $g_j^{\text{in}}$  are concave, e.g.,

if  $g_j^{\text{in}}$  are  $\chi$  functions. The next result shows that  $\chi$  functions defined over closed intervals are invariant through operator  $\Omega$  by solving (14) explicitly.

*Lemma 5:* If  $g_j^{\text{in}}$  is a  $\chi$  function (cf. (15)) with top point  $\tau_j = (\tau_j^1, \tau_j^2)$  and  $X_j = [q_j^l, q_j^u]$  ( $q_j^l \leq \tau_j^1 \leq q_j^u$ ) for all  $j \in [n]$ , then the following hold true for  $\Omega$  defined in (14):

- (i)  $g^{\text{out}} = \Omega\{(g_j^{\text{in}}, X_j)\}_{j \in [n]}$  is a  $\chi$  function with top point  $(\mathbf{1}^T \tau^1, \mathbf{1}^T \tau^2)$  and domain  $[\mathbf{1}^T q^l, \mathbf{1}^T q^u]$ .
- (ii) the set of maximizers is  $\{x^* \in [q^l, \tau^1] \mid \mathbf{1}^T x^* = z\}$  if  $\mathbf{1}^T q^l \leq z < \mathbf{1}^T \tau^1$ , is  $\{\tau^1\}$  if  $z = \mathbf{1}^T \tau^1$ , and is  $\{x^* \in [\tau^1, q^u] \mid \mathbf{1}^T x^* = z\}$  if  $\mathbf{1}^T \tau^1 < z \leq \mathbf{1}^T q^u$ .

where  $\tau^1 := \tau_{[n]}^1$ ,  $\tau^2 := \tau_{[n]}^2$ ,  $q^l := q_{[n]}^l$  and  $q^u := q_{[n]}^u$  are  $n$  dimensional vectors.

*Remark 12:* Lemma 4 implies that the condition  $\tau_j^1 \in X_j$  in Lemma 5 is without loss of generality. In addition, the top point of  $g^{\text{out}}$  is inside its domain, that is,  $\mathbf{1}^T \tau^1 \in [\mathbf{1}^T q^l, \mathbf{1}^T q^u]$ .

We now consider the case when  $X_j$  is the union of a finite number of disjoint intervals for all  $j \in [n]$ . Assume  $X_j$  contains  $m_j$  pieces of intervals and denote each piece by  $X_j^k$ , then  $X_j = \cup_{k=1}^{m_j} X_j^k$ . The way to solve the nonconvex problem (14) is to decompose it into multiple subproblems, where each subproblem is associated with a combination  $\sigma \in \Theta := \prod_{j=1}^n [m_j] \subset \mathbf{R}^n$  of intervals  $X_j^{\sigma_j}$  and is denoted by  $\Omega(\sigma) := \Omega\{(g_j^{\text{in}}, X_j^{\sigma_j})\}_{j \in [n]}$ . That is,

$$\Omega\{(g_j^{\text{in}}, X_j)\}_{j \in [n]} = \max_{\sigma \in \Theta} \Omega(\sigma) \quad (16)$$

If the restriction of  $g_j^{\text{in}}$  to  $X_j^k$  is a  $\chi$  function for all  $k \in [m_j]$  and  $j \in [n]$ , then Lemma 5 can be used to solve subproblems  $\Omega(\sigma)$  for all  $\sigma \in \Theta$ . This motivates the following definition of *piecewise  $\chi$  functions*.

*Definition 3:*  $g : X \subseteq \mathbf{R} \rightarrow \mathbf{R}$  is called a *piecewise  $\chi$  function* if the domain  $X$  is the union of multiple disjoint intervals, and over each of these intervals,  $g$  is a restricted  $\chi$  function.

*Remark 13:* The domain  $X$  of a piecewise  $\chi$  function, as defined in Definition 3, is not necessarily connected.

The next result shows that piecewise  $\chi$  functions are invariant through operator  $\Omega$ , whose proof follows straightforwardly from (16), Lemma 5, Remark 12 and the fact that the point-wise maximum of multiple  $\chi$  functions is a piecewise  $\chi$  function.

*Proposition 2:* If, for all  $j \in [n]$ ,  $X_j \subset \mathbf{R}$  is the union of disjoint and closed intervals (including rays) and  $g_j^{\text{in}} : X_j \rightarrow \mathbf{R}$  is a piecewise  $\chi$  function, then  $\Omega\{g_j^{\text{in}}, X_j\}_{j=1}^n$  is a piecewise  $\chi$  function.

The number of subproblems on the right hand side of (16) can be large. The next result provides conditions under which the number of subproblems required to be considered in (16) can be significantly decreased. This is illustrated in Example 3.

*Proposition 3:* For all  $j \in [n]$ , let  $X_j \subset \mathbf{R}$  be the union of disjoint and closed intervals (including rays) and let  $g_j^{\text{in}} : \text{conv } X_j \rightarrow \mathbf{R}$  be a  $\chi$  function with top point  $\tau_j = (\tau_j^1, \tau_j^2)$ . Then  $\Omega\{(g_j^{\text{in}}, X_j)\}_{j \in [n]} = \Omega\{(g_j^{\text{in}}, \text{conv } X_j)\}_{j \in [n]}$  if and only if (1)  $\tau_j^1 \in X_j$  for all  $j \in [n]$ ; and (2) both  $\sum_{j=1}^n X_j \cap (-\infty, \tau_j^1]$  and  $\sum_{j=1}^n X_j \cap [\tau_j^1, \infty)$  are connected sets.

*Example 3:* Consider the following quantities. Let  $X_1 = [-4, -2] \cup [-1.5, 1.5] \cup [2, 4]$ ,  $X_2 = [-4, 4]$ , and  $X_3 = [-4, -2] \cup [-1, 1] \cup [2, 4]$ . Let  $g_i : X_i \rightarrow \mathbf{R}$ ,  $i \in [3]$ , be piecewise  $\chi$  functions.  $g_1$  contains four pieces:  $\chi_{(-3,4)}$  over  $[-4, -2]$ ,  $\chi_{(-1,2)}$  over  $[-1.5, 0]$ ,  $\chi_{(1,2)}$  over  $(0, 1.5]$ , and  $\chi_{(3,4)}$  over  $[4, 2]$ .  $g_2$  contains two pieces  $\chi_{(-3,4)}$  over  $[-4, 0]$  and  $\chi_{(3,4)}$  over  $(0, 4]$ .  $g_3$  has the same values as  $g_1$  over its domain. Let  $g_i^{\text{out}} = \Omega(\{g_{i,j}^{\text{in}}, X_{i,j}\}_{j \in [2]}$ , where  $g_{i,j}^{\text{in}} = g_i$  and  $X_{i,j} = X$  for  $j \in [2]$  and  $i \in [3]$ .

Application of Proposition 3 can be illustrated using the above quantities as follows. Computing  $g_1^{\text{out}}$  requires solving 16 subproblems according to (16). However, following Proposition 3, it is sufficient to consider only 4 subproblems. This is because  $g_1^{\text{out}} = g_2^{\text{out}}$  and computing  $g_2$  requires solving 4 subproblems. The proof for  $g_1^{\text{out}} = g_2^{\text{out}}$  is as follows: first, since  $g_3 \leq g_1 \leq g_2$ ,<sup>7</sup> it is straightforward to see from (14) that  $g_3^{\text{out}} \leq g_1^{\text{out}} \leq g_2^{\text{out}}$ ; then, Proposition 3 implies that  $g_3^{\text{out}} = g_2^{\text{out}}$ .

#### IV. AN EQUIVALENT STATE AGGREGATION APPROACH

The computational approach proposed in Section III has provable guarantees only for tree reducible networks. In this section, we return to the approach outlined in Section II-D, and (9) in particular, for a general network topology. We recall that, in its current form, (9) is not amenable to implementations because the underlying state space is uncountably infinite. In this section, we develop an equivalent finite abstraction of the state space through *state aggregation*, and correspondingly develop an aggregated version of (9).

##### A. A State Aggregation Approach

The key idea is to develop a finite *consistent partition* of one time step reachable sets. We recall a few standard terminologies. A *cover* of a set  $S$  is a collection of nonempty subsets  $\{S_i\}_{i \in I}$  of  $S$  such that  $S = \cup_{i \in I} S_i$  and a *partition* is a cover with pairwise disjoint elements. We call a cover or partition finite if it contains finitely many elements. Furthermore, for a network

<sup>7</sup>We use the convention that the values at undefined points are  $-\infty$ .

state  $(\mathcal{E}, p)$ , a partition  $\{S_i\}_{i \in I}$  of set  $S \subseteq \mathcal{B}_{\mathcal{E}}$  is said to be *consistent* if,  $\mathcal{F}_{\mathcal{E}}(\mathcal{E}, u) = \mathcal{F}_{\mathcal{E}}(\mathcal{E}, \tilde{u})$  for all  $u, \tilde{u} \in S_i, i \in I$ . Consistency implies that it is valid to write  $\mathcal{F}_{\mathcal{E}}(\mathcal{E}, u) \equiv \mathcal{F}_{\mathcal{E}}(\mathcal{E}, S_i)$  for all  $u \in S_i$  and  $i \in I$ . Note here that the set  $S_i$  is not necessarily the set of admissible control actions  $U(\mathcal{E}, p)$ , and can be any arbitrary set of balanced supply-demand vectors. We extend the notion of the set of admissible control actions (5) as follows: for a link set  $\mathcal{E}$  and a set  $P \subseteq \mathcal{B}_{\mathcal{E}}$ ,

$$U(\mathcal{E}, P) := \cup_{p \in P} U(\mathcal{E}, p) = \mathcal{B}_{\mathcal{E}} \cap \text{cube } P \quad (17)$$

where  $\text{cube } P := \cup_{p \in P} \text{cube } p$ .

A finite consistent partition of the set of control actions induces a natural finite cover of the reachable state space at each stage in the cascading dynamics. At  $t = 0$ , the state space  $\{(\mathcal{E}^0, p^0)\}$  is a singleton, and therefore  $\{(\mathcal{E}^0, P^0)\}$  forms a trivial partition with  $P^0 := \{p^0\}$ . Let  $\{U_i^0\}_{i \in I_1}$  be a finite consistent partition of  $U(\mathcal{E}^0, P^0)$ . Then at  $t = 1$ , the reachable state space  $\{(\mathcal{F}_{\mathcal{E}}(\mathcal{E}^0, u), u) \mid u \in U(\mathcal{E}^0, p^0)\}$  is covered by  $\{(\mathcal{E}_i^1, P_i^1)\}_{i \in I_1} = \{(\mathcal{F}_{\mathcal{E}}(\mathcal{E}^0, U_i^0), U_i^0)\}_{i \in I_1}$ . Let  $\{U_j^1\}_{j \in I_2^i}$  be a finite consistent partition of  $U(\mathcal{E}_i^1, P_i^1)$ , for all  $i \in I_1$ . Then at  $t = 2$ , the state space reachable from  $(\mathcal{E}_i^1, P_i^1), \{(\mathcal{F}_{\mathcal{E}}(\mathcal{E}_i^1, u), u) \mid u \in U(\mathcal{E}_i^1, P_i^1)\}$ , is covered by  $\{(\mathcal{E}_j^2, P_j^2)\}_{j \in I_2^i} = \{(\mathcal{F}_{\mathcal{E}}(\mathcal{E}_i^1, U_j^1), U_j^1)\}_{j \in I_2^i}$ , for all  $i \in I_1$ . Repeated application of this procedure to all the subsequent stages then gives the desired finite representation. We employ the elements  $(\mathcal{E}^t, P^t)$  of the cover at time  $t$  as aggregated states. A natural extension of (4) to dynamics over the aggregated states is as follows:

$$(\mathcal{E}^{t+1}, P^{t+1}) = \mathcal{F}(\mathcal{E}^t, P^t, U^t), \quad U^t \in \mathbb{U}(\mathcal{E}^t, P^t) \quad (18)$$

where  $\mathcal{F}_p(\mathcal{E}, P, U) \equiv \mathcal{F}_p(U) := U$  and  $\mathcal{F}_{\mathcal{E}}(\mathcal{E}, P, U) \equiv \mathcal{F}_{\mathcal{E}}(\mathcal{E}, U) := \{i \in \mathcal{E} \mid |f_i(\mathcal{E}, u)| \leq c_i, \forall u \in U\}$ .  $\mathbb{U}(\mathcal{E}^t, P^t)$  is defined by the particular choice of consistent partition of  $U(\mathcal{E}^t, P^t)$ , and serves as the set of admissible aggregated control actions at state  $(\mathcal{E}^t, P^t)$ . We associate  $\mathcal{E}$  with a vector  $\beta \in \{1, 0, -1\}^{\mathcal{E}}$ .  $\beta_i$  is used to denote whether the flow capacity constraint of link  $i \in \mathcal{E}$  is satisfied or not: the flow stays within capacities for  $\beta_i = 0$  and exceeds the upper and lower capacities for  $\beta_i = 1$  and  $\beta_i = -1$ , respectively. Let  $U(\mathcal{E}, P, \beta) := \{u \in U(\mathcal{E}, P) \mid f_i(\mathcal{E}, u) < -c_i \text{ for } \beta_i = -1; |f_i(\mathcal{E}, u)| \leq c_i \text{ for } \beta_i = 0; f_i(\mathcal{E}, u) > c_i \text{ for } \beta_i = 1; \forall i \in \mathcal{E}\}^8$ . The consistent partition used in this paper is:

$$\mathbb{U}(\mathcal{E}, P) := \{U(\mathcal{E}, P, \beta) \mid \beta \in \{1, 0, -1\}^{\mathcal{E}}\} \setminus \emptyset \quad (19)$$

<sup>8</sup>See Remark 14 for a variant definition of  $U(\mathcal{E}, P, \beta)$ .

If  $U(\mathcal{E}, P)$  is a polytope, then each member of  $\mathbb{U}(\mathcal{E}, P)$  is also a polytope, with possibly half open boundary due to the strict inequalities in  $U(\mathcal{E}, P, \beta)$ . An algorithmic procedure to compute and store the partition  $\mathbb{U}$  defined in (19) will be presented in Section V.

State aggregation gives a finite tree (cf. Section II-D), whose nodes are aggregated states and arcs are aggregated control actions. The set of feasible aggregated states is  $\mathbb{S} := \{(\mathcal{E}, P) \mid (\mathcal{E}, p) \in \mathcal{S}, \forall p \in P\}$  and the reward associated with a state  $(\mathcal{E}, P) \in \mathbb{S}$  is  $\sup_{p \in P} s^\top p = \max_{p \in \text{cl}(P)} s^\top p$ , where  $\text{cl}(P)$  denotes the closure of  $P$ . The optimal search over the aggregated tree can be performed through the following calculations, which are adaptations of (9):

$$\mathbb{J}_1(\mathcal{E}, P) = \max_{u \in U(\mathcal{E}, \text{cl}(P))} s^\top u \quad \text{s.t.} \quad |f(\mathcal{E}, u)| \leq c_{\mathcal{E}} \quad (20a)$$

$$\mathbb{J}_{t+1}(\mathcal{E}, P) = \max_{U \in \mathbb{U}(\mathcal{E}, P)} \mathbb{J}_t(\mathcal{F}_{\mathcal{E}}(\mathcal{E}, U), U) \quad (20b)$$

where  $t \in [N - 1]$  and  $\mathbb{J}_t(\mathcal{E}, P)$  is the maximum among values of all feasible aggregated states that can be reached in at most  $t$  time steps starting from  $(\mathcal{E}, P)$ . Similar to (9a), the flow constraint is imposed in (20a) to ensure the additional constraint on  $u^{N-1}$  (cf. Remark 2). This implies that the unique (and optimal) aggregated control action associated with  $\mathbb{J}_1(\mathcal{E}, P)$  is  $U^{N-1,*} = U(\mathcal{E}, P, \mathbf{0})$ . This is to be contrasted with (20b) for  $t \geq 2$  that the optimal aggregated control action  $U^{t,*}$  is not trivial to obtain. (20a) maximizes a linear function over a bounded closed set and (20b) maximizes over the finite set  $\mathbb{U}(\mathcal{E}, P)$ . Therefore, the optimal value is achievable in every iteration in (20). The next result shows that the iterations in (20) give the same value as that in (9).

*Theorem 1:* Consider a network with initial state  $(\mathcal{E}^0, p^0)$ , link weights  $w \in \mathbf{R}_{\geq 0}^{\mathcal{E}^0}$  and link capacities  $c \in \mathbf{R}_{\geq 0}^{\mathcal{E}^0}$ . For every aggregated state  $(\mathcal{E}, P)$  obtained from the consistent partition in (19), the computations in (9) and (20) satisfy the following for  $t \in [N]$ :

$$\mathbb{J}_t(\mathcal{E}, P) = \sup_{p \in P} J_t(\mathcal{E}, p)$$

*Proof:* We prove by induction. For  $t = 1$ :  $\sup_{p \in P} J_1(\mathcal{E}, p) = \sup_{p \in P} \max_{u \in U(\mathcal{E}, p)} \{s^\top u \mid |f(\mathcal{E}, u)| \leq c_{\mathcal{E}}\} = \mathbb{J}_1(\mathcal{E}, P)$ . Suppose the claim is true for  $t \in [k]$ .

$$\begin{aligned} \mathbb{J}_{k+1}(\mathcal{E}, P) &= \max_{U \in \mathbb{U}(\mathcal{E}, P)} \mathbb{J}_k(\mathcal{F}_{\mathcal{E}}(\mathcal{E}, U), U) \\ &= \max_{U \in \mathbb{U}(\mathcal{E}, P)} \sup_{u \in U} J_k(\mathcal{F}_{\mathcal{E}}(\mathcal{E}, u), u) = \sup_{u \in U(\mathcal{E}, P)} J_k(\mathcal{F}_{\mathcal{E}}(\mathcal{E}, u), u) \\ &= \sup_{p \in P} \sup_{u \in U(\mathcal{E}, p)} J_k(\mathcal{F}_{\mathcal{E}}(\mathcal{E}, u), u) = \sup_{p \in P} J_{k+1}(\mathcal{E}, p) \end{aligned}$$

where the first equality is due to (20b); the second equality is due to the induction assumption; the third and fourth equalities are due to  $\cup_{U \in \mathbb{U}(\mathcal{E}, P)} U = U(\mathcal{E}, P) = \cup_{p \in P} U(\mathcal{E}, p)$ , as implied by the definitions of  $\mathbb{U}(\mathcal{E}, P)$  and  $U(\mathcal{E}, P)$ ; and the last equality is due to (9). ■

We make the following remarks on the state aggregation and aggregated tree search.

*Remark 14:*

- 1) Every path of length  $N$  in the aggregated search tree corresponds to a, possibly different, topology sequence that can occur in the cascading dynamics. The state aggregation proposed here is the minimal among all finite abstractions for exact computation of optimal control.
- 2) It is straightforward to see from (20) that the value of  $\mathbb{J}_t(\mathcal{E}, P)$  depends only on  $\text{cl}(P)$  for all  $t \in [N]$ . Therefore, without introducing error in the computation of  $\mathbb{J}_t(\mathcal{E}, P)$ , we use  $(\mathcal{E}, \text{cl}(P))$  and  $\text{cl}(U)$  in place of  $(\mathcal{E}, P)$  and  $U$ . Correspondingly, without stating explicitly, hereafter we use the following variant of the definition in (19):  $U(\mathcal{E}, P, \beta) := \{u \in U(\mathcal{E}, P) \mid f_i(\mathcal{E}, u) \leq -c_i \text{ if } \beta_i = -1; |f_i(\mathcal{E}, u)| \leq c_i \text{ if } \beta_i = 0; f_i(\mathcal{E}, u) \geq c_i \text{ if } \beta_i = 1; \forall i \in \mathcal{E}\}$ .

### B. Optimal Control Synthesis: From Aggregated to the Original State Space

The numerical implementation of (20) is shown in Section V. Given such a procedure to compute  $U^* = (U^{0,*}, \dots, U^{N-1,*})$ , we next present a result to derive  $u^* = (u^{0,*}, \dots, u^{N-1,*})$ , i.e., control actions for the cascading failure dynamics in (4) over the unaggregated state space. However, since the set of feasible control action sequences  $\mathcal{D}$  is not necessarily closed (cf. Remark 2), finding  $u^*$  whose cost is *exactly* the same as that of  $U^*$  may not be possible. It is however possible to find  $u^*$  whose cost is arbitrarily close to that of  $U^*$ .

*Proposition 4:* For a network with initial state  $(\mathcal{E}^0, p^0)$ , link weights  $w \in \mathbf{R}_{\geq 0}^{\mathcal{E}^0}$ , and link capacities  $c \in \mathbf{R}_{\geq 0}^{\mathcal{E}^0}$ , consider  $\mathbb{J}_N(\mathcal{E}^0, \{p^0\})$  computed by (20). For every  $\epsilon > 0$ , there exists  $\tilde{u} \in \mathcal{D}$  such that  $\mathbb{J}_N(\mathcal{E}^0, \{p^0\}) \geq s^T \tilde{u}^{N-1} \geq \mathbb{J}_N(\mathcal{E}^0, \{p^0\}) - \epsilon$ .

*Proof:* For brevity, in this proof, we let  $\mathbb{J}_N(\mathcal{E}^0, \{p^0\}) \equiv \mathbb{J}_N(\mathcal{E}^0, p^0)$ . Theorem 1 implies that  $\mathbb{J}_N(\mathcal{E}^0, p^0) = J_N(\mathcal{E}^0, p^0) \geq s^T u^{N-1}$  for all  $u \in \mathcal{D}$ . Therefore, we only prove the second inequality.

Let  $U^*$  be an optimal aggregated control sequence associated with computing  $\mathbb{J}_N(\mathcal{E}^0, p^0)$  in (20), and let  $\mathcal{E}^*$  be the induced active link set sequence (recall  $U^{N-1,*} = U(\mathcal{E}^{N-1,*}, U^{N-2,*}, \mathbf{0})$ ). Let  $u^{N-1,*}$  be a maximizer to (20a) for  $\mathbb{J}_1(\mathcal{E}^{N-1,*}, U^{N-2,*})$ . Then,  $u^{N-1,*} \in \text{cl}(U^{N-1,*})$  and

$\mathbb{J}_N(\mathcal{E}^0, p^0) = s^T u^{N-1,*}$ . We now show that, for arbitrary  $\epsilon > 0$ , there exists  $\tilde{u} \in \mathcal{D}$  such that  $s^T \tilde{u}^{N-1} \geq s^T u^{N-1,*} - \epsilon$ .

Let  $M(u, \epsilon)$  be the open ball centered at  $u \in \mathbf{R}^{\mathcal{V}}$  with radius  $\epsilon$ . Since  $u^{N-1,*} \in \text{cl}(U^{N-1,*})$ ,  $U^{N-1,*} \cap M(u^{N-1,*}, \epsilon/|\mathcal{V}_l|) \neq \emptyset$  for every  $\epsilon > 0$ . It is then possible to pick  $\tilde{u}^{N-1} \in U^{N-1,*} \cap M(u^{N-1,*}, \epsilon/|\mathcal{V}_l|)$  such that  $\tilde{u}^{N-1} \neq u^{N-1,*}$  and  $s^T \tilde{u}^{N-1} > s^T u^{N-1,*} - \epsilon$ . It is now sufficient to show that there exist  $\tilde{u}^0, \tilde{u}^1, \dots, \tilde{u}^{N-2}$  such that  $\tilde{u}^{t+1} \in \text{cube } \tilde{u}^t$  and  $\tilde{u}^t \in U^{t,*}$  for all  $0 \leq t \leq N-2$ . We provide details for  $\tilde{u}^{N-2}$ ; the reasoning for  $\tilde{u}^{N-3}, \dots, \tilde{u}^0$  follows along the same lines.

Since  $u^{N-1,*} \in U(\mathcal{E}^{N-1,*}, \text{cl}(U^{N-2,*}))$ , there exists  $u^{N-2,*} \in \text{cl}(U^{N-2,*})$  such that  $u^{N-1,*} \in \text{cube } u^{N-2,*}$ . Hence, we can pick  $\tilde{u}^{N-2} \in U^{N-2,*} \cap M(u^{N-2,*}, \|u^{N-1,*} - \tilde{u}^{N-1}\|_2)$  so that  $\tilde{u}^{N-2} \neq u^{N-2,*}$  and  $\tilde{u}^{N-1} \in \text{cube } \tilde{u}^{N-2}$ , where the special choice of  $\tilde{u}^{N-1} \neq u^{N-1,*}$  ensures that  $M(u^{N-2,*}, \|u^{N-1,*} - \tilde{u}^{N-1}\|_2)$  has positive radius. ■

The proof of Proposition 4 implies that, in order to find  $u^*$ , it remains to solve for  $u^{N-1,*}$  from (20a). The next result implies that (20a) is a linear program by showing that, for every  $(\mathcal{E}, P)$ , the set  $U(\mathcal{E}, P)$  is a polytope.

*Lemma 6:* Consider a network with initial state  $(\mathcal{E}^0, p^0)$ , link weights  $w \in \mathbf{R}_{\geq 0}^{\mathcal{E}^0}$  and link capacities  $c \in \mathbf{R}_{\geq 0}^{\mathcal{E}^0}$ . For every aggregated state  $(\mathcal{E}^t, P^t)$ ,  $t \in [N] \cup \{0\}$ , induced by the consistent partition in (19), both  $P^t$  and  $U(\mathcal{E}^t, P^t)$  are polytopes.

*Proof:* The claim is proved by induction. It is easy to see that  $P^0 = \{p^0\}$  and  $U(\mathcal{E}^0, P^0) = U(\mathcal{E}^0, p^0)$  are polytopes. Suppose  $P^t$  and  $U(\mathcal{E}^t, P^t)$  are polytopes for some  $t \in [N-1] \cup \{0\}$ . It is sufficient to show that, for arbitrary aggregated control action  $U \in \mathbb{U}(\mathcal{E}^t, P^t)$ , the resulting  $P^{t+1}$  and  $U(\mathcal{E}^{t+1}, P^{t+1})$  are polytopes.  $P^{t+1} = U^t = U(\mathcal{E}^t, P^t, \beta)$  for some  $\beta \in \{-1, 0, +1\}^{\mathcal{E}^t}$  (cf. (19)). Combining this with the induction assumption that  $U(\mathcal{E}^t, P^t)$  is a polytope, we get that  $P^{t+1}$  is a polytope. It follows from the definition in (17) that  $U(\mathcal{E}^{t+1}, P^{t+1})$  is a polytope as well. ■

*Remark 15:*

- 1) Combined with the definition of cube  $P$ , the proof of Lemma 6 also implies that, for every  $(\mathcal{E}, P)$ , both  $P$  and  $U(\mathcal{E}, P)$  are contained in a closed orthant of  $\mathbf{R}^{\mathcal{V}_l}$ .
- 2) The aggregated tree search based on (20) can be interpreted as a systematic way to decompose the nonconvex feasible set  $\mathcal{D} \subset \mathbf{R}^{N \times |\mathcal{V}|}$  in (7)-(8) into a finite number of subsets. Each subset is a polytope and corresponds to a topology sequence and aggregated control sequence. For example, the subset corresponding to  $(U^0, \dots, U^{N-1})$  is  $\Pi_{t=0}^{N-1} U^t$ . Similar

to (16), the optimal value of (7) is equal to the maximum among the optimal values of multiple subproblems associated with the subsets. Each subproblem is a linear program of the form  $\sup_{u \in \Pi_{t=0}^{N-1} U^t} s^T u^{N-1}$  and indeed coincides with (20a).

- 3) The state aggregation approach allows to include running cost into the problem formulation. In that case, instead of a linear program, a dynamic program is to be solved for every  $(U^0, \dots, U^{N-1})$ .

### C. Efficient Aggregated Tree Search

With (18) and (19) specifying how to expand nodes of aggregated network state and (20) directing the goal of search, one can then employ any classical tree search algorithm, e.g., the ones in [24, Chap 3], to solve the problem. Regarding the implementation of tree search algorithms, a few remarks are in order. First, the following relationship can be used for tree pruning in a standard branch and bound algorithm framework.

$$\mathbb{J}_1(\mathcal{E}, P) \leq \mathbb{J}_t(\mathcal{E}, P) \leq \max_{p \in \text{cl}(P)} s^T p \quad \forall (\mathcal{E}, P), \forall t \in [N]$$

Second, iterative deepening depth-first search algorithm presents several advantages for the optimal control problem. On one hand, it achieves a good balance between time and space complexities. This is of particular importance because the number of aggregated states in the optimal control problem can be quite large. On the other hand, the search can be stopped anytime in the process of computation while producing a feasible control action with reasonable performance. In fact, the search over the first  $t < N$  layer provides an optimal  $t$ -stage load shedding scheme. At the same time, the upper bound provides an estimate of performance gap from the optimal value when search is terminated early.

Third, following (3) and (19), going from one node to another in the aggregated search tree involves computation of pseudo-inverse of Laplacian associated with the new active link set. Doing such a computation from scratch for every search move could be computationally expensive, particularly for large  $\mathcal{E}^0$  or for large  $N$ . This problem can be addressed by incrementally updating pseudo-inverse of the Laplacian under link removal, e.g., see [12], [27], [28].

Finally, while the detailed search algorithm including pruning is standard and omitted here, its implementation with set objects, i.e., the aggregated control action  $U \in \mathbb{U}(\mathcal{E}, P)$  and the set  $\mathbb{U}(\mathcal{E}, P)$ , require additional tools. Section V is devoted to this particular problem.

## V. COMPUTING AGGREGATION THROUGH ARRANGEMENT OF HYPERPLANES

The numerical implementation of (20) relies critically on proper representation of set  $U(\mathcal{E}, P)$  and its partition  $\mathbb{U}(\mathcal{E}, P)$ . While Lemma 6 characterizes an important property of these objects, in this section, we provide an algorithmic procedure for their representation. Our machinery relies on and extends tools from the domain of *arrangement of hyperplanes* e.g., see [17] [18, Chapter 24], and *polytopes*, e.g., see [19] [20].

### A. Arrangement, Polytope and Incidence Graph

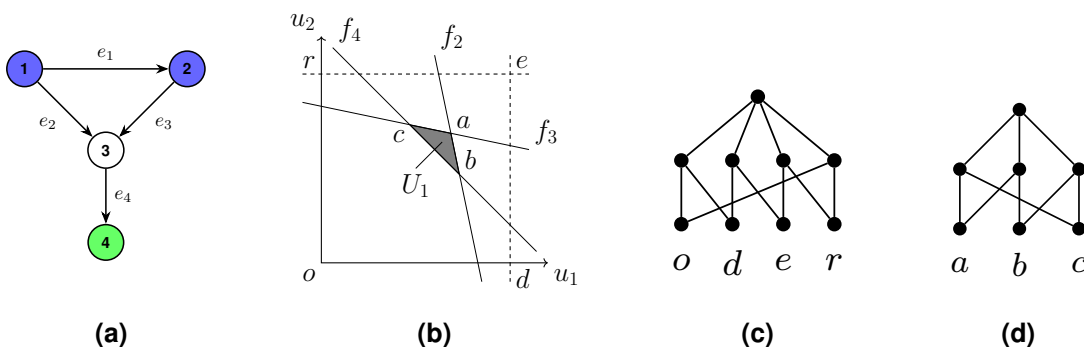


**Fig. 5:** (a) a network  $(\mathcal{V}, \mathcal{E}^0)$  with  $\mathcal{V}_+ = \{1, 2\}$ ,  $\mathcal{V}_- = \{4\}$ ,  $w = \mathbf{1}$ ,  $c = [10, 3, 3, 6]^T$ ,  $p^0 = [-5, -5, 0, 10]^T$ ; (b) projections of  $U(\mathcal{E}^0, p^0)$  and  $\{u \in \mathcal{B}_{\mathcal{E}^0} \mid f_i(\mathcal{E}^0, u) = c_i\}$ ,  $i \in \{2, 3, 4\}$ , on  $u_1 - u_2$  plane; (c) incidence graph of  $U(\mathcal{E}^0, p^0)$ ; (d) incidence graph of  $U_1$ .

We start with the simple illustrative example shown in Fig. 5a. Referring to the definition of cube  $p^0$ , there are three non-trivial components of  $p^0$ . Taking into account the additional constraint imposed by  $\mathcal{B}_{\mathcal{E}}$ , referring to (5), the set of admissible control actions  $U(\mathcal{E}^0, p^0)$  can be completely understood in terms of its two dimensional projection, say on the  $u_1 - u_2$  plane. In Fig. 5b, the box  $oder$  and the point  $e$  correspond to the projections of  $U(\mathcal{E}^0, p^0)$  and  $p^0$ , respectively, and the solid lines labeled by  $f_2, f_3, f_4$  correspond to the projections of capacity constraints associated with the links  $e_2, e_3$  and  $e_4$ . The flow capacity constraint for  $e_1$  is ignored here because it is satisfied by all  $u \in U(\mathcal{E}^0, p^0)$  and hence irrelevant for the problem. Lines  $f_2, f_3$  and  $f_4$  dissect the box  $oder$  into seven two dimensional pieces. Each piece, e.g., the triangle  $abc$  denoted by  $U_1$ , is an aggregated control action, e.g.,  $U_1 = U(\mathcal{E}^0, p^0, [0, 0, 0, 1]^T)$ . These seven pieces constitute the partition  $\mathbb{U}(\mathcal{E}^0, \{p^0\})$ .

In general, a finite collection  $\mathcal{H}$  of hyperplanes in  $\mathbf{R}^d$  dissects  $\mathbf{R}^d$  into finitely many connected pieces of various dimensions. The collection of these pieces is called the *arrangement*, denoted

by  $\mathcal{A}(\mathcal{H})$ , induced by  $\mathcal{H}$ , and each piece is called a *face*, denoted by  $\Gamma$ , of the arrangement. The dimension of a face is the dimension of its affine hull; a  $k$  dimensional face is called a  $k$ -face, denoted by  $\Gamma^k$ . For convenience, 0-face, 1-face,  $(d-2)$ -face,  $(d-1)$ -face and  $d$ -face are, respectively, referred to as *vertex*, *edge*, *ridge*, *facet* and *cell*<sup>9</sup>. We call two faces *incident* if one is contained in the boundary of the other and if the difference in their dimensions is one. In a pair of incident faces, the lower (or higher) dimensional face is called the subface (or superface) of the other. In Fig. 5b, the three solid lines (i.e., hyperplanes) dissect box *oder* into seven cells, nine edges (or facets) and three vertices (or ridges). As indicated by this example, in the setting of this paper, for every state  $(\mathcal{E}, P)$ , the capacity constraints, balanced condition (captured by  $\mathcal{B}_{\mathcal{E}}$ ), and load shedding requirement (captured by  $\text{cube}(P)$ ) form the collection of hyperplanes. We are interested in the substructure of the arrangement of these hyperplanes inside  $U(\mathcal{E}, P)$ . The closure of each facet in the substructure corresponds to an aggregated control action and the collection of these facets corresponds to  $\mathbb{U}(\mathcal{E}, P)$ <sup>10</sup>.

The closure of a bounded face in the arrangement is a polytope, or polytope for short. We use the same letter  $P$ , as in the aggregated state, to denote a general polytope for simplicity, because every aggregated state is a polytope, as shown in Lemma 6. Formally, a *polytope* is a point set  $P \subset \mathbf{R}^d$  that can be presented either as a convex hull of a finite number of points in  $\mathbf{R}^d$  or the bounded intersection of finite number of closed half spaces in  $\mathbf{R}^d$  [19]. The same notion of face, as in an arrangement, is used for a polytope  $P \subset \mathbf{R}^d$ <sup>11</sup> and furthermore, a face of  $P$  can be described as  $\Gamma = P \cap \{x \in \mathbf{R}^d \mid \pi^T x = \pi_0\}$ , where the linear inequality  $\pi^T x \leq \pi_0$  must be satisfied for all  $x \in P$ . We call  $P \subset \mathbf{R}^d$  full dimensional if its dimension is  $d$ . For a full dimensional polytope, the affine hull of its facet  $\Gamma_i^{d-1}$  is a hyperplane, denoted by  $H_i = \{x \in \mathbf{R}^d \mid (\pi^i)^T x = \pi_0^i\}$  and referred as its *defining hyperplane*. As a convention, the direction of  $\pi^i$  for  $H_i$  is chosen to point outwards from  $P$ .

The geometry of the arrangement of hyperplanes and polytopes is difficult to comprehend, especially in high dimensions. Because of this, they are represented using *incidence graph* (also

<sup>9</sup>In some literature, *cell* is used to refer to the connected pieces and *face* is used exclusively for the 2-face. In this paper, we adopt the terminology convention in [17] and use *cell* to denote  $d$ -face exclusively in  $\mathbf{R}^d$ .

<sup>10</sup>Fig. 5b shows the projection of the arrangement in  $\mathbf{R}^3$  onto the  $u_1 - u_2$  plane. Each cell in Fig. 5b is the projection of a facet of the arrangement.

<sup>11</sup>The notion of *face* is slightly different for an arrangement and a polytope. While the former considers a face as an open set, the latter treats a face as a closed set. This difference does not affect the results in this section and hence ignored.

called the *facial lattices* or *face lattices*). The incidence graph of an arrangement or a polytope contains the incidence relationship between various faces. It is a layered (undirected) graph whose nodes have a one-to-one correspondence with faces of the arrangement or polytope, and an edge exists between two nodes if and only if the corresponding faces are incident. All the nodes corresponding to faces of the same dimension constitute a layer. We place the layer corresponding to vertices at the bottom, and the layer corresponding to cells on the top. For example, Fig. 5c shows the incidence graph of the polytope *oder* (or projection of  $U(\mathcal{E}^0, p^0)$ ). The single node at the top layer corresponds to *oder* itself, the four nodes in the middle layer correspond to the four edges *or*, *re*, *ed* and *do*, and the four nodes in the bottom layer correspond to the four vertices *o*, *r*, *e* and *d*. The edges between these layers correspond to the incidence relation between the faces, as shown in Figure 5b. Similarly, 5d shows the incidence graph of the polytope *acb* (or aggregated control action  $U_1$ ).

Furthermore, we have the following remark on the auxiliary information required for storing the incidence graph of an arrangement or a polytope.

*Remark 16:* When implemented, the incidence graph is usually associated with some auxiliary information that enables numerical implementation of geometric operations such as determining if a hyperplane intersects with a face, or finding the intersection of a hyperplane and an edge. Further details can be found, e.g., in [29] and [17]. While several choices for auxiliary information are possible, in this paper, we use the following: analytical expressions for hyperplanes, coordinate for vertices, and for every face, the mean of the coordinates of the vertices contained in it. We shall not explicitly mention this auxiliary information in algorithms in subsequent sections.

### B. Constructing the Incidence Graph of $U(\mathcal{E}, P)$ and $\mathbb{U}(\mathcal{E}, P)$

We recall from Section IV that the implementation of (20) relies on an efficient procedure to construct the representations (i.e., incidence graphs) of  $U(\mathcal{E}, P)$  and  $\mathbb{U}(\mathcal{E}, P)$  from that of  $P$ . Such a procedure starts with the incidence graph of  $P^0 = \{p^0\}$ , which is known trivially, and is to be repeatedly invoked at every iteration in (20). The procedure consists of two steps: (I) construct the incidence graph of cube  $P$  from that of  $P$ , and (II) construct the incidence graph of  $U(\mathcal{E}, P)$  and  $\mathbb{U}(\mathcal{E}, P)$  from that of cube  $P$ . The key ingredient in step (II) is a sub-procedure to update incidence of graph of cube  $P$  upon addition of hyperplanes corresponding to  $\mathcal{B}_{\mathcal{E}}$  (cf. (17)) and flow capacity constraints to get  $U(\mathcal{E}, P)$  and  $\mathbb{U}(\mathcal{E}, P)$  respectively. Implementation

of such a sub-procedure exists in well-known algorithms for constructing arrangement of an arbitrary set of hyperplanes, e.g., in [30] and [17, Chapter 7]. On the other hand, to the best of our knowledge, a systematic algorithmic description to execute step (I) does not exist in the literature. The purpose of Section V-C is to address this deficiency.

*Remark 17:*

- 1) The algorithms in [30] and [17, Chapter 7] have time complexity  $\Theta(|\mathcal{H}|^d)$  for constructing a general positioned arrangement of hyperplanes in  $\mathcal{H}$  in a  $d$  dimensional affine space. Note for a connected network with active link set  $\mathcal{E}$ ,  $U(\mathcal{E}, P)$  is contained in the  $|\mathcal{V}_l| - 1$  dimensional affine space  $\mathcal{B}_{\mathcal{E}} \cap \{p \in \mathbf{R}^{\mathcal{V}} \mid p_i = 0, \forall i \in \mathcal{V} \setminus \mathcal{V}_l\}$ .
- 2) For a network with a single supply-demand pair, the hyperplanes and aggregated controls reduce to points and contiguous intervals that can be represented by two numbers. In this case,  $\text{cube}(P)$  can be computed in constant time: e.g., for  $P = (p^l, p^u] \subset \mathbf{R}_{\geq 0}$ ,  $\text{cube}(P) = [0, p^u]$ ; and the incidence graph of  $\mathbb{U}(\mathcal{E}, P)$  at every state  $(\mathcal{E}, P)$  can be computed in linear time with respect to the number of infeasible links.
- 3) Recalling that  $\tilde{\mathcal{D}}_i$  defined in (10) is for a (sub-)network  $\mathcal{G}_i$  between a single supply-demand pair, the procedure in 2) of this remark can be used for its construction.  $\tilde{\mathcal{D}}_i$  is the set of feasible aggregated control sequences without monotonicity constraint. Therefore, when constructing the incidence graph for the set  $\mathbb{U}(\mathcal{E}, P)$  of aggregated controls at state  $(\mathcal{E}, P)$ , instead of building upon  $\text{cube } P$ , one needs to use  $[-c^{\text{min-cut}}, c^{\text{min-cut}}]$ , where  $c^{\text{min-cut}}$  is the min-cut capacity of  $\mathcal{G}_i$ . Similarly, when constructing  $\tilde{\mathcal{D}}_i$  for constant control (as used in Section III-C), one needs to use  $P$  rather than  $\text{cube } P$ .

### C. Constructing the Incidence Graph of $\text{cube } P$ from the Incidence Graph of $P$

Remark 15 implies that it is sufficient to focus on  $P \subset \mathbf{R}_{\geq 0}^d$ . We first consider  $\text{cube } p^0$  for  $p^0 \in \mathbf{R}_{\geq 0}^d$ . Since the dimensions corresponding to  $p_i^0 = 0$  can be ignored, we assume  $p^0 \in \mathbf{R}_{> 0}^d$  without loss of generality. In this case,  $\text{cube } p^0 \subset \mathbf{R}_{\geq 0}^d$  is a hypercube and its incidence graph can be obtained straightforwardly by Lemma 7, whose proof is omitted. Fig. 5c shows an example in  $\mathbf{R}^2$ .

*Lemma 7:* For  $p^0 \in \mathbf{R}_{> 0}^d$ , let  $\alpha : \text{cube } p^0 \rightarrow \{-1, 0, 1\}^d$  be defined as:  $\alpha_i(x) = -1$  if  $x_i = 0$ ,  $\alpha_i(x) = 0$  if  $x_i \in (0, p_i^0)$ , and  $\alpha_i(x) = 1$  if  $x_i = p_i^0$ . Then,

- (i) every  $\tilde{\alpha} \in \{-1, 0, 1\}^d$  is associated with a  $(d - |\tilde{\alpha}|_1)$ -face  $\Gamma(\tilde{\alpha}) := \text{cl}(\{x \in \text{cube } p^0 \mid \alpha(x) = \tilde{\alpha}\})$  of  $\text{cube } p^0$ ;

(ii) two faces  $\Gamma(\alpha^1)$  and  $\Gamma(\alpha^2)$  of cube  $p^0$  are incident if  $\alpha^1$  and  $\alpha^2$  are equal except for one component which equals zero in one among  $\alpha^1$  and  $\alpha^2$ .

*Remark 18:* Lemma 7 (i) describes a procedure to enumerate all the nodes in the incidence graph of cube  $p^0$ , in terms of all vectors in  $\{-1, 0, 1\}^d$ , whereas (ii) specifies how to add edges to the incidence graph.

For a general polytope  $P \subset \mathbf{R}_{\geq 0}^d$ , we present a sequential procedure to construct the incidence graph of cube  $P$  from that of  $P$ . For this purpose, we define the *projection* and *sweep* of a polytope  $P \subset \mathbf{R}_{\geq 0}^d$  in direction  $\mathbf{e}_k$ ,  $k \in [d]$ :

$$\text{proj}_k(P) := \{p - p_k \mathbf{e}_k \mid p \in P\} \quad (21)$$

$$\text{sweep}_k(P) := \{p - \theta_k p_k \mathbf{e}_k \mid p \in P, \theta_k \in [0, 1]\} \quad (22)$$

It is straightforward that  $P \subseteq \text{sweep}_k(P)$  and  $\text{proj}_k P \subseteq \text{sweep}_k(P)$ . In fact,  $\text{sweep}_k(P)$  is the trace of  $P$  projecting to  $\text{proj}_k P$  in the direction of  $\mathbf{e}_k$  and therefore, it is also a polytope in  $\mathbf{R}_{\geq 0}^d$ . One can again apply sweep on  $\text{sweep}_k(P)$  along  $\mathbf{e}_i$  for some  $i \neq k$  and get  $\text{sweep}_i(\text{sweep}_k(P)) = \{p - \theta_1 p_k \mathbf{e}_k - \theta_2 p_i \mathbf{e}_i \mid p \in P, (\theta_1, \theta_2) \in [0, 1]^2\}$ . This motivates us to define sweep for an index set  $I \subseteq [d]$  as

$$\text{sweep}_I(P) := \left\{ p - \sum_{k \in I} \theta_k p_k \mathbf{e}_k \mid p \in P, \theta_k \in [0, 1] \forall k \in I \right\}.$$

With this definition, cube  $P = \text{sweep}_{[d]}(P)$  can be obtained by recursively applying sweep on  $P$ , e.g.,

$$\text{sweep}_{[d]}(P) = \text{sweep}_1(\text{sweep}_2(\dots \text{sweep}_d(P))).$$

Therefore, in order to obtain cube  $P$ , it is sufficient to focus on constructing  $\text{sweep}_k(P)$  from  $P$  for a given  $k \in [d]$ .

Let  $\bar{H} := \{x \in \mathbf{R}^d \mid x_k = 0\}$  and  $\bar{H}^+ := \{x \in \mathbf{R}^d \mid x_k \geq 0\}$ .<sup>12</sup> For a given polytope  $P \subset \bar{H}^+$  and  $k \in [d]$ ,  $\text{sweep}_k(P)$  relates to projection between two affine spaces:  $\text{aff } P \subset \mathbf{R}^d$  and  $\text{aff } \text{proj}_k P \subset \bar{H}$ . We differentiate between the following two scenarios based on the difference in dimensions of these two affine spaces: (I)  $\dim P = \dim(\text{proj}_k P)$ ; and (II)  $\dim P = \dim(\text{proj}_k P) + 1$ . Scenario I occurs when  $P$  is contained in a hyperplane that is not orthogonal to  $\bar{H}$ . In this case, there is a one-to-one correspondence between the points in  $P$

<sup>12</sup>We do not show subscript  $k$  for brevity in notation.

and  $\text{proj}_k P$ . Scenario II occurs when either  $\dim P = d$ , or every hyperplane containing  $P$  is orthogonal to  $\bar{H}$ . The two scenarios are illustrated in Figure 6 for  $\mathbf{R}^2$  and  $k = 2$ .

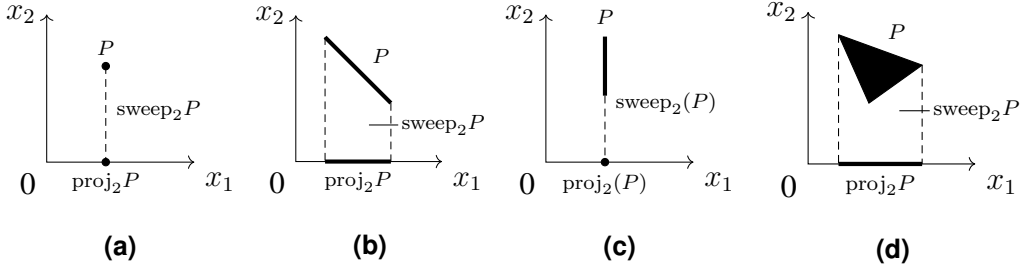


**Fig. 6:** Two possible scenarios for projection: (a) and (b) show the projection onto a space of the same dimension; and (c) and (d) show projection onto a space of lower dimension.

### Scenario I

In this scenario,  $\text{proj}_k(P)$  is *affinely isomorphic*<sup>13</sup> to  $P$ . Therefore, its incidence graph is identical to that of  $P$ . The following result relates the incidence graph of  $\text{sweep}_k(P)$  to that of  $P$  and  $\text{proj}_k(P)$ .

*Proposition 5:* Consider an  $n$  dimensional polytope  $P \subset \{x \in \mathbf{R}^d \mid x_k > 0\}$ ,  $0 \leq n \leq d - 1$ . If there exists a hyperplane containing  $P$  which is not orthogonal to  $\bar{H}$ , then: (i)  $\text{sweep}_k(P)$  is an  $(n + 1)$  dimensional polytope; (ii) an  $l$ -face of  $\text{sweep}_k(P)$  is either an  $l$ -face of  $P$  or of  $\text{proj}_k P$ , or it is  $\text{sweep}_k \Gamma^{l-1}$  for some  $(l - 1)$ -face  $\Gamma^{l-1}$  of  $P$ ; and (iii) each face of  $P$  and of  $\text{proj}_k P$  is a face of  $\text{sweep}_k(P)$ , and  $\text{sweep}_k \Gamma$  is a face of  $\text{sweep}_k P$  for every face  $\Gamma$  of  $P$ .

*Proof:* Let  $\hat{\gamma} := 1.2 \max_{x \in P} x_k$ . Since  $P$  is contained in a hyperplane that is not orthogonal to  $\bar{H}$ , the line segment  $[0, \hat{\gamma} \mathbf{e}_k]$  is not parallel to  $\text{aff } P$ . Let  $\hat{P} := P - [0, \hat{\gamma} \mathbf{e}_k]$ . We have the following facts on  $\hat{P}$  [20, Chapter 4.4]:  $\hat{P}$  is an  $(n + 1)$  dimensional polytope; an  $l$ -face of  $\hat{P}$  is either an  $l$ -face of  $P$  or of  $P - \{\hat{\gamma} \mathbf{e}_k\}$ , or it is the Minkowski sum of singleton  $-\{\hat{\gamma} \mathbf{e}_k\}$  and some  $(l - 1)$ -face of  $P$ ; each face of  $P$  and of  $P - \{\hat{\gamma} \mathbf{e}_k\}$  is a face of  $\hat{P}$ ; and the Minkowski sum of singleton  $-\{\hat{\gamma} \mathbf{e}_k\}$  and any face of  $P$  is a face of  $\hat{P}$ .

It is then sufficient to show that  $\text{sweep}_k P$  and  $\hat{P}$  are combinatorial isomorphic<sup>14</sup>. By definition,

<sup>13</sup>Two polytopes  $P_1 \subseteq \mathbf{R}^{d_1}$  and  $P_2 \subseteq \mathbf{R}^{d_2}$  are *affinely isomorphic* to each other if there exists an affine and bijection map between them.

<sup>14</sup>Two polytopes  $P_1$  and  $P_2$  are *combinatorial isomorphic* to each other if there exists a one-to-one correspondence  $\varphi$  between the set of faces in  $P_1$  and the set of faces in  $P_2$ , such that  $\varphi$  is inclusion-preserving, i.e., for two faces  $\Gamma_1$  and  $\Gamma_2$  of  $P_1$ ,  $\Gamma_1 \subset \Gamma_2$  if and only if  $\varphi(\Gamma_1) \subset \varphi(\Gamma_2)$ .

$\text{sweep}_k(P) = \hat{P} \cap \bar{H}^+$ . The correspondence between face  $\hat{\Gamma}$  of  $\hat{P}$  and face  $\tilde{\Gamma}$  of  $\text{sweep}_k(P)$  is as follows:  $\tilde{\Gamma} = \hat{\Gamma}$  if  $\hat{\Gamma} \subset \{x \in \mathbf{R}^d \mid x_k > 0\}$ ;  $\tilde{\Gamma} = \text{proj}_k(\hat{\Gamma})$  if  $\hat{\Gamma} \subset \{x \in \mathbf{R}^d \mid x_k < 0\}$ ; and  $\tilde{\Gamma} = \hat{\Gamma} \cap \bar{H}^+$  otherwise. ■

*Remark 19:* The complement of the  $P \subset \{x \in \mathbf{R}^d \mid x_k > 0\}$  condition in Proposition 5 can be handled as follows. If  $P \subset \bar{H}$ , then trivially  $\text{sweep}_k(P) = P = \text{proj}_k(P)$ . For the remaining scenario when  $P \cap \bar{H} \neq \emptyset$ , one can use a standard perturbation trick [17]. Let  $\hat{P}$  be a small perturbation of  $P$  such that  $\hat{P} \subset \{x \in \mathbf{R}^d \mid x_k > 0\}$ , and hence to which Proposition 5 applies. The incidence graph of  $P$  is then obtained from that of  $\hat{P}$  by merging faces which are in close proximity (relative to the perturbation) and maintaining incidence relationships between the remaining faces.

Example 4 illustrates how to use Proposition 5 to obtain the incidence graph of  $\text{sweep}_k(P)$  in  $\mathbf{R}^2$ .

*Example 4:* Consider the polytope  $P$  corresponding to the line segment between points  $a$  and  $b$  in Figure 7a. The figure also shows the corresponding  $\hat{P}$ ,  $\text{proj}_2(P)$  and  $\text{sweep}_2(P)$ . The subgraph shown in solid black in Figure 7b is the incidence graph of  $P$ , whereas the subgraph shown in gray, which is identical to the solid black one, is the incidence graph of  $\text{proj}_2 P$ , where  $a' = \text{proj}_2(a)$ ,  $b' = \text{proj}_2(b)$ . The incidence graph of  $\text{sweep}_2(P)$  is constructed using Proposition 5 as follows:

- 1) The vertices (0-faces) contain vertices both of  $P$ , i.e.,  $a$  and  $b$ , and of  $\text{proj}_2(P)$ , i.e.,  $a'$  and  $b'$ ;
- 2) The edges (1-faces) contain both the edge of  $P$ , i.e.,  $ab$ , the edge of  $\text{proj}_2(P)$ , i.e.,  $a'b'$ , and the edges formed by sweep of vertices, i.e.,  $aa'$  and  $bb'$ ;
- 3) Edges  $aa'$  and  $bb'$  are incident to  $a, a'$  and  $b, b'$ , respectively, as they result from sweeping, contain the corresponding vertices, and their dimensions differ by 1;
- 4)  $\text{sweep}_2(P)$  is a two dimensional polytope. Its incidence graph contains itself as a 2-face incident to all the edges.

## Scenario II

For the second scenario, we first identify the faces of  $P$  that play a role in the projection and then resort to Proposition 5 for construction of  $\text{sweep}_k(P)$ . It is sufficient to consider  $P \subset \mathbf{R}_{\geq 0}^d$  to be full dimensional, i.e.,  $\dim P = d$ . Otherwise, one can work in the affine space  $\text{aff } P$ , which is orthogonal to  $\bar{H}$ , and the same results hold. Let  $\Gamma_i^{d-1}$  be a facet of  $P \subset \bar{H}^+$ , recall that the

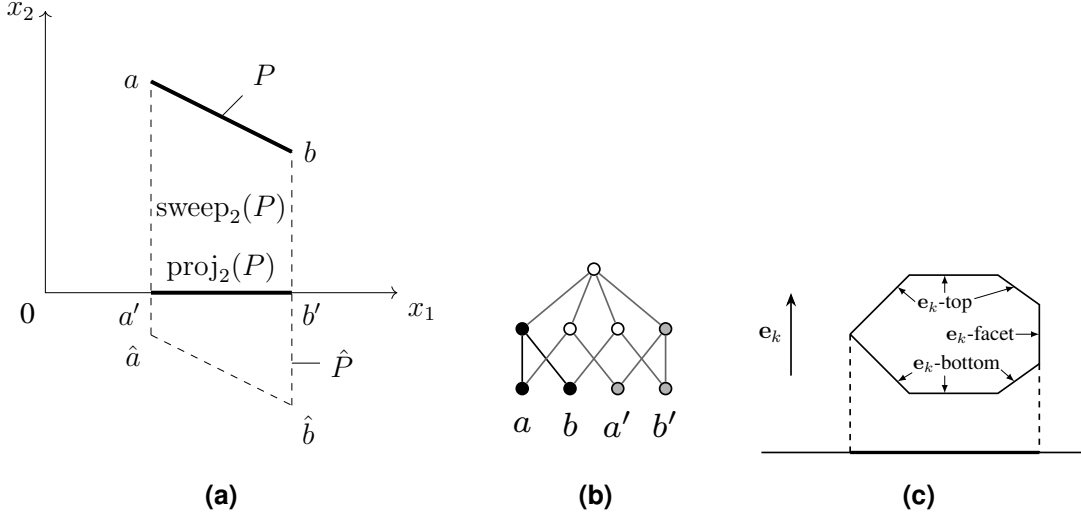


**Fig. 7:** (a) a sample polytope  $P$  in  $\mathbf{R}^2$ , its sweep, projection, and related objects; (b) the incidence graph of  $\text{sweep}_2(P)$ ; and (c) different facets according to the direction  $\mathbf{e}_k$

direction of  $\pi^i$  for its defining hyperplane  $H_i$  is pointed outwards from the polytope. A direction vector  $\mu \in \mathbf{R}^d$  classifies the facets of  $P$  into three types [31] according to the value of  $\mu^\top \pi^i$ :  $\mu$ -facet for  $\mu^\top \pi^i = 0$ ,  $\mu$ -bottom for  $\mu^\top \pi^i < 0$  and  $\mu$ -top for  $\mu^\top \pi^i > 0$ . With this definition, a facet  $\Gamma^i$  belongs to  $\mathbf{e}_k$ -top if  $\pi_k^i > 0$ ,  $\mathbf{e}_k$ -facet if  $\pi_k^i = 0$  and  $\mathbf{e}_k$ -bottom if  $\pi_k^i < 0$ . This is illustrated in Figure 7c.

The  $\mathbf{e}_k$ -top and  $\mathbf{e}_k$ -bottom facets can be described as the facets that are “visible from the direction  $-\mathbf{e}_k$ ” and “visible from the direction  $\mathbf{e}_k$ ”, respectively. For the projection concerned in  $\text{sweep}_k(P)$ , only points in  $\mathbf{e}_k$ -top play a role. This is straightforward to see in  $\mathbf{R}^2$  and  $\mathbf{R}^3$ . For example, the top vertex of the vertical edge in Fig. 6c and the top edge of the triangular face in 6d completely determine the sweeps. In general, Proposition 6 shows the same is true for  $\mathbf{R}^d$ , where we say point  $x \in \mathbf{R}^d$  is *shaded* by point  $\hat{x} \in \mathbf{R}^d$  in direction  $\mathbf{e}_k$  if  $\hat{x}_k \geq x_k$  and  $\hat{x}_i = x_i$  for all  $i \in [d] \setminus \{k\}$ . It is clear from the definition that a point plays no role in the projection along  $\mathbf{e}_k$  if it is shaded by another point of  $P$  in  $\mathbf{e}_k$ . The ridges in  $\mathbf{e}_k$ -top facet of  $P$  are of two types: one is in the intersection between two  $\mathbf{e}_k$ -top facets, and the other is in the intersection between a  $\mathbf{e}_k$ -top facet and either a  $\mathbf{e}_k$ -facet or a  $\mathbf{e}_k$ -bottom facet. Proposition 6 implies that the second type of ridges determine the boundaries of  $\text{sweep}_k(P)$  and  $\text{proj}_k(P)$ . They are hence called *boundary ridges* of  $P$  in direction  $\mathbf{e}_k$ .

*Proposition 6:* For a full dimensional polytope  $P \subset \bar{H}^+$  and  $k \in [d]$ , the following are true:

- (i) every point in  $P$  is shaded in direction  $\mathbf{e}_k$  by a point in a  $\mathbf{e}_k$ -top facet of  $P$ ;
- (ii) every  $\mathbf{e}_k$ -top facet is a facet of  $\text{sweep}_k(P)$ ; and
- (iii) for a ridge  $\Gamma^{d-2}$  of  $P$ ,  $\text{sweep}_k(\Gamma^{d-2})$  is a facet of  $\text{sweep}_k(P)$  if and only if  $\Gamma^{d-2}$  is a boundary ridge and  $\Gamma^{d-2} \not\subseteq \bar{H}$ .

With Proposition 5 and Proposition 6, cube  $P$  of a full dimensional polytope  $P \subset \mathbf{R}_{\geq 0}^d$  can be constructed as follows: set  $k = 1$ ; while  $k \leq d$ , do the following:

- (I) find  $\mathbf{e}_k$ -top facets of  $P$  and remove all faces of  $P$  that are not contained in any of them;
- (II) find the boundary ridges and construct their sweep along  $\mathbf{e}_k$  according to Proposition 5 and Remark 19;
- (III) add a facet in  $\bar{H}$  that is incident to the projections of all boundary ridges along  $\mathbf{e}_k$  and a cell, corresponding to  $\text{sweep}_k(P)$ , that is incident to all the facets;
- (IV) set  $P = \text{sweep}_k(P)$ ,  $k = k + 1$ , and repeat;

where the second step is possible because every boundary ridge belongs to a  $\mathbf{e}_k$ -top facet that is not orthogonal to  $\bar{H}$ . The above four-step procedure is illustrated in Example 5.

*Example 5:* Consider  $P = U_1 \subset \mathbf{R}_{\geq 0}^2$  shown in Fig. 5b, in this case cube  $U_1 = \text{sweep}_1(\text{sweep}_2(U_1))$ . These two sweep operations are shown in Fig. 8a and 8c, respectively. In particular, Fig. 8b shows the incidence graph of  $\text{sweep}_2(U_1)$ , where the solid black substructure is inherited from the incidence graph of  $U_1$ . As can be seen, the  $\mathbf{e}_2$ -bottom facet  $cb$  is removed in  $\text{sweep}_2(U_1)$ ; the  $\mathbf{e}_2$ -top facets, edges  $ac$  and  $ab$ , and the associated subfaces, vertices  $a, b, c$ , persist; the boundary ridges, vertices  $b$  and  $c$ , play critical roles in the construction of  $\text{sweep}_2(U_1)$ : their projections, i.e.,  $b'$  and  $c'$ , and sweeps, i.e.,  $bb'$  and  $cc'$ , are added as ridges and facets, respectively.

*Remark 20:* If  $(\mathcal{E}, P)$  has multiple connected components, then it is efficient to construct incidence graphs for each component separately, using the technique presented in this section. However, one first needs to construct the incidence graph for the projection of  $P$  onto the subspace associated with every component. For a component that does not contain nodes  $\{i, \dots, j\}$ , the corresponding projection is obtained iteratively as  $\text{proj}_i(\dots \text{proj}_j(P))$ . The required operations on the incidence graph of  $P$  to execute these projections are already contained in Propositions 5 and 6.

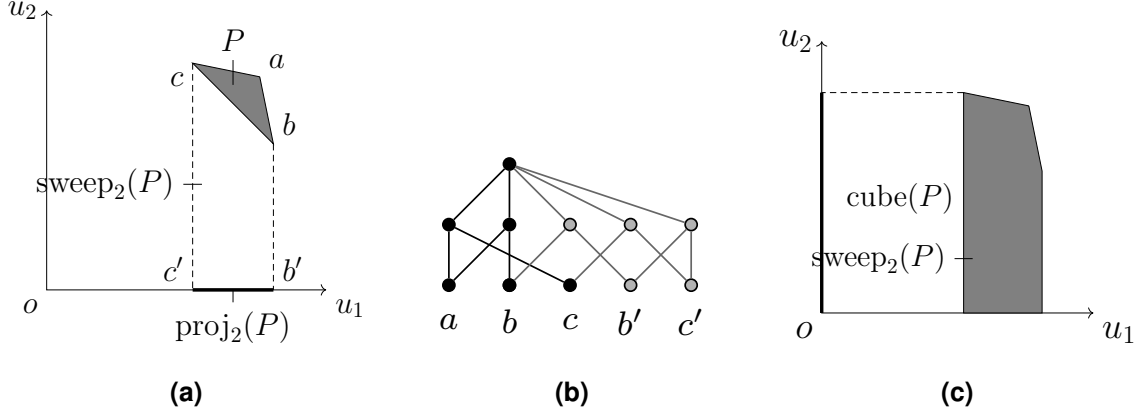


**Fig. 8:** Illustration of sweep: (a) sweep of  $U_1$ ; (b) the incidence graph of  $\text{sweep}_2(U_1)$ ; and (c)  $\text{cube } U_1$  as sweep of  $\text{sweep}_2(U_1)$ .

## VI. APPROXIMATION ALGORITHM AND SIMULATIONS

### A. Approximation Algorithm via Projection

The exponential dependence of the time complexity on  $d = |\mathcal{V}_l| - 1$  (see Remark 17) can be prohibitive for networks that contain large number of non-transmission nodes. We now outline a strategy to project the admissible control actions onto a lower dimensional space. Aggregation and search in the lower dimensional space then gives an approximation.

Consider a network  $\mathcal{G} = (\mathcal{V}, \mathcal{E})$  with supply-demand vector  $p$ . For the sake of presentation in this section, assume, without loss of generality that  $\mathcal{V} = \mathcal{V}_l$ , i.e., every node is a non-transmission node; if this is not the case, then one can focus only on the subspace of control actions corresponding to the non-transmission nodes. Let  $\Phi = [\Phi_1, \dots, \Phi_{|\mathcal{V}_l|}] \in \mathbf{R}^{|\mathcal{V}_l| \times |\mathcal{V}_l|}$  be an orthonormal (transformation) matrix, and let  $B \subset [|\mathcal{V}_l|]$  be an index set. The approximation strategy, which is parametrized by  $(\Phi, B)$ , considers aggregated set of admissible control actions in the subspace  $U(\mathcal{E}, P) \cap \mathcal{R}(\Phi_B) = \{u \in U(\mathcal{E}, P) \mid \Phi_i^T u = 0, i \notin B\}$ <sup>15</sup>, i.e., in the subspace of control actions which can be expressed as a linear combination of  $\Phi_i, i \in B$ . Remark 17 implies that this reduces the dimension, and hence correspondingly the time complexity, from  $|\mathcal{V}_l| - 1$  to  $|B|$ . Moreover, since the constraints  $\Phi_i^T u = 0, i \notin B$ , are hyperplanes, they can be easily integrated into the construction of arrangements to get  $\mathbb{U}(\mathcal{E}, P) \cap \mathcal{R}(\Phi_B)$ . In fact, by

<sup>15</sup> $\mathcal{R}(\Phi_B)$  denotes the range of matrix  $\Phi_B$ .

setting  $\Phi_i = \mathbf{1}/\sqrt{|\mathcal{V}_i|}$  for some  $i \notin B$ , the constraint  $\Phi_i^T u = 0$  is the balance constraint for a connected network (cf. (2)).

*Example 6:* Consider a network with initial supply-demand vector  $p^0$ . By choosing  $B = \{1\}$  and  $\Phi_1 = p^0/\|p^0\|_2$ , we get *proportional control policies* [10, Section 6.1.1], i.e., a class of control policies whose action set at state  $(\mathcal{E}, p)$  is  $\{\lambda p \mid 0 \leq \lambda \leq 1\}$ .

The one-dimensional search space resulting from proportional control policy, as shown in Example 6, is favorable for computational purposes. However, the projection-based approximation strategy implies that one could possibly find better control actions, using comparable computational budget, by using different projections. This is illustrated using simulations on IEEE 39 benchmark system in Section VI-B.

## B. Simulations

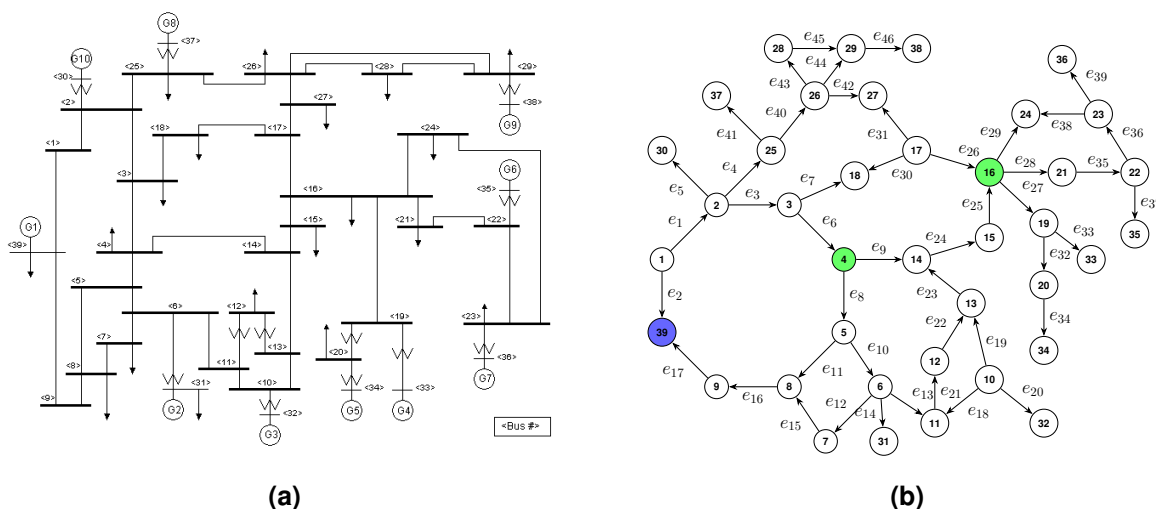


**Fig. 9:** (a) the IEEE 39 bus network from [32]; (b) simplified visualization of the network in (a), with the specific choice of supply and demand nodes used for simulations

We conducted numerical experiments on the IEEE 39 bus system illustrated in Figure 9. Node 39 is selected to be the only supply; nodes 4 and 16 are selected to be loads; all the other nodes are transmission nodes. This particular choice of supply-demand nodes is consistent with the fact that the actual supply and demand on these nodes, as reported in [32], have relatively large values.  $p^0$  was chosen to be proportional to the actual values reported in [32] for nodes 4, 16 and 39:  $p_4^0 = p_{16}^0 = -5$ ,  $p_{39}^0 = 10$  and  $p_i^0 = 0$  for all  $i \notin \{4, 16, 39\}$ . Link susceptances  $w$

are from [32]. The link capacities were selected as follows:  $c_8 = 0.5$ ,  $c_9 = 1$ ,  $c_i = 2.5$  for  $i \in \{13, 21, 22, 23\}$ ;  $c_i = 3.0$  for  $i \in \{3, 28, 29, 35, 36, 38\}$ ;  $c_i = 3.5$  for  $i \in \{16, 17\}$ ;  $c_i = 4.0$  for  $i \in \{7, 26, 30\}$ ;  $c_i = 4.5$  for  $i \in \{1, 2, 4, 24, 25, 31, 39, 40, 42\}$  and  $c_i = 2.0$  for other links.

**TABLE I:** Optimal residual load under (7) and under the projection-based approximations in (23)

$N \backslash \eta$	0	0.1	0.2	0.3	0.4	0.5	0.6	0.7	0.8	0.9	1	Optimal
1	3.716	3.502	3.310	3.140	2.984	2.844	2.718	2.600	2.494	2.396	2.304	3.716
2	9.860	9.806	9.750	9.696	8.974	9.000	7.334	6.742	4.578	4.078	4.000	9.860
3	10.000	11.112	11.090	11.028	10.000	9.000	7.334	6.742	5.000	4.444	4.000	11.150
4	10.000	11.112	11.090	11.028	10.000	9.000	7.334	6.742	5.000	4.444	4.000	11.150
5	10.000	11.112	11.090	11.028	10.000	9.000	7.334	6.742	5.000	4.444	4.000	11.150

For the above network parameters,  $(\mathcal{E}^0, p^0)$  is infeasible. Furthermore, under no load shedding control action, i.e.,  $u^t \equiv p^0$  for all  $t$ , the only supply node 39 would get disconnected at  $t = 1$  from the load nodes 4 and 16. However, using the control formulation of this paper, such a scenario can be prevented while minimizing the amount of load to be shed. Table I (last column) shows the values of residual load, i.e., the optimal solution to (7), computed by the techniques in Section V, for different control horizons  $N$ . The residual load is expectedly nondecreasing with  $N$ . This confirms that multi-round control does lead to increase in the residual load, or equivalently decrease in cumulative load shed, in comparison to the single round ( $N = 1$ ) control underlying power re-dispatch. However, there are no gains in residual load beyond  $N \geq 3$ . This is because the network in Figure 9 contains a very few cycles; and once the network becomes a tree, the optimal load shedding action is to ensure feasibility of all the links in this case.

Table I also shows optimal residual load within the class of control policies obtained by projection onto a one-dimensional space, as described in Section VI-A. Specifically, we chose

$$B = \{1\}, \quad \Phi_1 \propto \eta \bar{p}^1 + (1 - \eta) \bar{p}^2, \quad \eta \in [0, 1] \quad (23)$$

where  $\bar{p}^1 \in \mathbf{R}^{39}$  has 1 and -1 on node 39 and 4, respectively, and 0 elsewhere;  $\bar{p}^2 \in \mathbf{R}^{39}$  has 1 and -1 on node 39 and 16, respectively, and 0 elsewhere. Recalling Example 6, it is easy to see that the set of proportional control policies [10, Section 6.1.1] corresponds to  $\eta = 0.5$ . Table I contains values for optimal residual load under such an approximation for different values of  $\eta$  and  $N$ . These values show that, similar to the optimal control actions, for every  $\eta$ , the optimal

residual load is nondecreasing in  $N$  and stays constant for  $N \geq 3$ . While there is no general monotone relationship in  $\eta$  (uniformly for all  $N$ ), the best control actions for  $N \geq 3$  correspond to  $\eta = 0.1$ . The control actions corresponding to  $\eta = 0.1$  perform uniformly better than the proportional control policy ( $\eta = 0.5$ ) which requires comparable computational cost, and give fairly similar performance as the optimal control actions which are obtained under considerable computational costs (Section V).

## VII. CONCLUSIONS AND FUTURE WORK

Cascading failure in physical networks has attracted great interest, and yet formal approaches for its control are relatively very few. This paper builds upon an existing formulation for optimal control of cascading failure in power networks under DC approximation, and provides approaches for computing optimal control in this setting. The decomposition paradigm and connections to computational geometry underlying our approaches suggest several avenues for future work.

As an initial step towards generalization, we plan to adapt the decomposition approach to be able to compute a feasible control action for non-tree reducible networks. We also plan to explore general optimal control formulations, beyond cascading failure and networked settings, to which the approaches developed in this paper are applicable. In particular, we plan to investigate connections between our approach of computing optimal control using (equivalent) finite representations and the recent work on symbolic optimal control, e.g., see [33].

## REFERENCES

- [1] R. Cohen, K. Erez, D. Ben-Avraham, and S. Havlin, “Resilience of the internet to random breakdowns,” *Physical review letters*, vol. 85, no. 21, p. 4626, 2000.
- [2] D. J. Watts, “A simple model of global cascades on random networks,” *PNAS*, vol. 99, no. 9, pp. 5766–5771, 2002.
- [3] A. Motter, “Cascade-based attacks on complex networks,” *Phys. Rev. E; Physical Review E*, vol. 66, no. 6, 2002.
- [4] P. Crucitti, V. Latora, and M. Marchiori, “Model for cascading failures in complex networks,” *Physical Review E*, vol. 69, no. 4, 2004.
- [5] A. Barrat, M. Barthelemy, and A. Vespignani, *Dynamical Processes on Complex Networks*. Cambridge University Press, 2008.
- [6] D. Bienstock, “Optimal control of cascading power grid failures,” in *Decision and Control and European Control Conference (CDC-ECC), 2011 50th IEEE Conference on*, pp. 2166–2173, IEEE, 2011.
- [7] K. Savla, G. Como, and M. A. Dahleh, “Robust network routing under cascading failures,” *IEEE Transactions on Network Science and Engineering*, vol. 1, no. 1, pp. 53–66, 2014.
- [8] D. Bienstock and A. Verma, “The n-k problem in power grids: New models, formulations, and numerical experiments,” *SIAM Journal on Optimization*, vol. 20, no. 5, pp. 2352–2380, 2010.

- [9] A. Bernstein, D. Bienstock, D. Hay, M. Uzunoglu, and G. Zussman, “Power grid vulnerability to geographically correlated failures: Analysis and control implications,” in *INFOCOM, 2014 Proceedings IEEE*, pp. 2634–2642, IEEE, 2014.
- [10] D. Bienstock, *Electrical Transmission System Cascades and Vulnerability: An Operations Research Viewpoint*, vol. 22. SIAM, 2016.
- [11] D. Braess, “Über ein paradoxon aus der verkehrsplanung,” *Unternehmensforschung*, vol. 12, no. 1, pp. 258–268, 1968.
- [12] Q. Ba and K. Savla, “A dynamic programming approach to optimal load shedding control of cascading failure in DC power networks,” in *IEEE Conference on Decision and Control*, (Las Vegas, NV), 2016.
- [13] C. Lai and S. H. Low, “The redistribution of power flow in cascading failures,” in *51st Annual Allerton Conference on Communication, Control, and Computing*, pp. 1037–1044, 2013.
- [14] L. Guo, C. Liang, and S. H. Low, “Monotonicity properties and spectral characterization of power redistribution in cascading failures,” *ACM SIGMETRICS Performance Evaluation Review*, vol. 45, no. 2, pp. 103–106, 2017.
- [15] J. Salmeron, K. Wood, and R. Baldick, “Analysis of electric grid security under terrorist threat,” *IEEE Transactions on power systems*, vol. 19, no. 2, pp. 905–912, 2004.
- [16] A. Pinar, J. Meza, V. Donde, and B. Lesieutre, “Optimization strategies for the vulnerability analysis of the electric power grid,” *SIAM Journal on Optimization*, vol. 20, no. 4, pp. 1786–1810, 2010.
- [17] H. Edelsbrunner, “Algorithms in combinatorial geometry, volume 10 of EATCS monographs on theoretical computer science,” 1987.
- [18] C. D. Toth, J. O’Rourke, and J. E. Goodman, *Handbook of discrete and computational geometry*. CRC press, 2004.
- [19] G. M. Ziegler, *Lectures on polytopes*, vol. 152. Springer Science & Business Media, 2012.
- [20] B. Grünbaum, V. Klee, M. A. Perles, and G. C. Shephard, *Convex polytopes*, vol. 16. Springer, 1967.
- [21] D. Halperin and M. Sharir, “Arrangements and their applications in robotics: recent developments,” in *Proceedings of the Workshop on Algorithmic Foundations of Robotics*, pp. 495–511, AK Peters, Ltd., 1995.
- [22] P. K. Agarwal, A. Efrat, S. K. Ganjugunte, D. Hay, S. Sankararaman, and G. Zussman, “The resilience of WDM networks to probabilistic geographical failures,” *IEEE/ACM Transactions on Networking*, vol. 21, no. 5, pp. 1525–1538, 2013.
- [23] Q. Ba and K. Savla, “Robustness of DC networks under controllable link weights,” *IEEE Transactions on Control of Network Systems*, 2017. In Press. Available at <http://arxiv.org/abs/1609.02179>.
- [24] S. J. Russell and P. Norvig, “Artificial intelligence: a modern approach (3rd edition),” 2009.
- [25] J. Chen, J. S. Thorp, and I. Dobson, “Cascading dynamics and mitigation assessment in power system disturbances via a hidden failure model,” *International Journal of Electrical Power and Energy Systems*, vol. 27, no. 4, pp. 318–326, 2005.
- [26] S. Boyd, N. Parikh, E. Chu, B. Peleato, and J. Eckstein, “Distributed optimization and statistical learning via the alternating direction method of multipliers,” *Foundations and Trends in Machine Learning*, vol. 3, no. 1, pp. 1–122, 2011.
- [27] S. Soltan, A. Loh, and G. Zussman, “Analyzing and quantifying the effect of  $k$ -line failures in power grids,” *IEEE Transactions on Control of Network Systems*, 2017. In press.
- [28] Q. Ba, *Elements of Robustness and Optimal Control for Infrastructure Networks*. PhD thesis, UNIVERSITY OF SOUTHERN CALIFORNIA, 2018. Available at <http://www-bcf.usc.edu/~ksavla/papers/Qin-thesis-main.pdf>.
- [29] M. De Berg, O. Cheong, M. Van Kreveld, and M. Overmars, *Computational Geometry: Introduction*. Springer, 2008.
- [30] H. Edelsbrunner, J. O’Rourke, and R. Seidel, “Constructing arrangements of lines and hyperplanes with applications,” *SIAM Journal on Computing*, vol. 15, no. 2, pp. 341–363, 1986.
- [31] T. Burger, P. Gritzmann, and V. Klee, “Polytope projection and projection polytopes,” *The American mathematical monthly*, vol. 103, no. 9, pp. 742–755, 1996.
- [32] R. D. Zimmerman, C. E. Murillo-Sánchez, and R. J. Thomas, “Matpower: Steady-state operations, planning, and analysis tools for power systems research and education,” *Power Systems, IEEE Transactions on*, vol. 26, no. 1, pp. 12–19, 2011.

- [33] M. Rungger and G. Reissig, “Arbitrarily precise abstractions for optimal controller synthesis,” in *IEEE Conf. on Decision and Control*, (Melbourne, Australia), 2017.
- [34] R. Sanyal and G. M. Ziegler, “Construction and analysis of projected deformed products,” *Discrete & Computational Geometry*, vol. 43, no. 2, pp. 412–435, 2010.
- [35] S. Boyd and L. Vandenberghe, *Convex optimization*. Cambridge university press, 2004.

## APPENDIX

### PROOFS

#### A. Proof of Proposition 1

We consider the following cases:

- 1)  $p_1^0 \leq R_{|\mathcal{E}|}$ . Remark 6 implies that  $(\mathcal{E}, p^0) \in \mathcal{S}$ . The optimal control for every  $N \geq 1$  would be shedding no load. In this case, by definition  $N_j(p^0) = 1$  for all  $j \in [\text{end}]$ . Every  $N \geq 1$  satisfies  $N_1(p^0) \leq N < N_0(p^0)$ . Hence,  $u^{*,t} = \min\{R_{o_1}, p_1^0\}[1 - 1]$  for  $t \geq 0$ . Since  $p_1^0 \leq R_{|\mathcal{E}|} \leq R_{o_1}$ ,  $u^*$  is optimal.
- 2)  $R_{o_{k+1}} < p_1^0 \leq R_{o_k}$  for some  $0 \leq k \leq \text{end} - 1$ . By definition,  $N_1(p^0) = N_2(p^0) = \dots = N_k(p^0)$  and  $N_{k+1}(p^0) \geq \dots \geq N_{\text{end}-1}(p^0) \geq 2 > N_{\text{end}}(p^0) = 1$ . We have the following cases.
  - a)  $N = 1$ . Since  $N_{\text{end}}(p^0) \leq 1 \leq N_{\text{end}-1}(p^0)$ ,  $u^* = \min\{R_{o_{\text{end}}}, p_1^0\}[1 - 1] = R_{|\mathcal{E}|}[1 - 1]$  is optimal, where the second equality follows from  $p_1^0 > R_{o_{k+1}} \geq R_{o_{\text{end}}} = R_{|\mathcal{E}|}$ .
  - b)  $N \geq N_k$ . In this case,  $N_1(p^0) \leq N < N_0(p^0)$ . Since  $p_1^0 \leq R_{o_k} \leq R_{o_1}$ ,  $u^{t,*} = p^0$  for all  $t$ .  $u^*$  is optimal if feasible. The latter is a straightforward result from the definition of  $N_k(p^0)$ .
  - c)  $2 \leq N < N_k$ . In this case,  $N_j(p^0) \leq N < N_{j-1}(p^0)$  for some  $k+1 \leq j \leq \text{end} - 1$ . Therefore,  $p_1^0 > R_{o_{k+1}} \geq R_{o_j}$ .  $u^{*,t} = p^0$  for  $0 \leq t < N_j(p^0) - 2$  and  $u^{t,*} = R_{o_j}[1 - 1]$  for  $N_j(p^0) - 2 \leq t \leq N - 1$ . We first show that  $u^* \in \mathcal{D}(\mathcal{E}, p^0, N)$ . Let  $(\mathcal{E}^0, \dots, \mathcal{E}^N)$  be the topology sequence under  $u^*$ . It is straightforward that  $(\mathcal{E}^0, \dots, \mathcal{E}^{N_j(p^0)-2}) = (\mathcal{E}_{\text{un}}^0, \dots, \mathcal{E}_{\text{un}}^{N_j(p^0)-2})$ . By definition of  $N_j(p^0)$ ,  $[o_j] \subset \mathcal{E}_{\text{un}}^{N_j(p^0)-2} = \mathcal{E}^{N_j(p^0)-2}$ . In addition, Remark 6 implies  $([o_j], R_{o_j}[1 - 1]) \in \mathcal{S}$  and, plus the definition of  $o_j$  further implies that  $([l], p^0) \notin \mathcal{S}$  for all  $l > o_j$ . Therefore,  $\mathcal{E}^t = [o_j]$  for all  $t \geq N_j(p^0) - 1$  and  $u^* \in \mathcal{D}(\mathcal{E}, p^0, N)$ . We then show optimality of  $u^*$  through contradiction. Suppose there exists a control  $\tilde{u} \in \mathcal{D}(\mathcal{E}, p^0, N)$  such that  $R_{o_j} < \tilde{u}_1^{N-1} \leq p_1^0$ . Let  $(\tilde{\mathcal{E}}^0, \dots, \tilde{\mathcal{E}}^{N-1})$  be the topology sequence under control  $\tilde{u}$ . Remark 4 implies that  $\mathcal{E}_{\text{un}}^{N-1} \subseteq \tilde{\mathcal{E}}^{N-1}$ . At the same

time, since  $N < N_{j-1}(p^0)$ ,  $\mathcal{E}_{\text{un}}^{N-1} \supseteq \mathcal{E}_{\text{un}}^{N_{j-1}(p^0)-2} \supset [o_{j-1}]$ . Note that the last inclusion is strict. Therefore,  $[o_{j-1}] \subset \tilde{\mathcal{E}}^{N-1}$ . Remark 6, combined with the definition of  $o_j$  and the assumption that  $\tilde{u}_1^{N-1} > R_{o_j}$ , implies that  $(\tilde{\mathcal{E}}^{N-1}, \tilde{u}^{N-1}) \notin \mathcal{S}$ . This contradicts with  $\tilde{u}$  being feasible.

### B. Proof of Lemma 5

First of all, it is clear that (14) is feasible only for  $z \in [\mathbf{1}^\top q^l, \mathbf{1}^\top q^u]$ . Secondly, since  $g_j^{\text{in}}$  is concave and  $X_j$  is convex, (14) is convex and strong duality holds. Therefore, it is sufficient to consider the dual problem in order to solve (14). Let  $\mu \in \mathbf{R}$  be the Lagrange multiplier associated with the constraint  $z = \mathbf{1}^\top x$ . The dual function is then given by:

$$\begin{aligned} \phi(\mu) &= -\mu z + \max_{q^l \leq x \leq q^u} \sum_{j=1}^n (\chi_{\tau_j}(x_j) + \mu x_j) \\ &= -\mu z + \sum_{j=1}^n \max_{q_j^l \leq x_j \leq q_j^u} (\chi_{\tau_j}(x_j) + \mu x_j) \\ &= \left( \sum_{j=1}^n x_j^*(\mu) - z \right) \mu + \sum_{j=1}^n \chi_j(x_j^*(\mu)) \end{aligned}$$

where  $x_j^*(\mu) \in \mathcal{X}_j^*(\mu) := \operatorname{argmax}_{q_j^l \leq x_j \leq q_j^u} (\chi_{\tau_j}(x_j) + \mu x_j)$ , for all  $j \in [n]$ .

For  $\mu \in [-1, 1]$ ,  $\chi_{\tau_j}(x_j) + \mu x_j$  is piecewise affine: nondecreasing with slope  $(1 + \mu)$  over  $(-\infty, \tau_j^1]$  and nonincreasing with slope  $(\mu - 1)$  over  $(\tau_j^1, +\infty)$ . Therefore,  $\tau_j^1 \in \mathcal{X}_j^*(\mu)$  for all  $\mu \in [-1, 1]$  and  $j \in [n]$ . This implies that  $\phi(\mu)$  is affine over  $[-1, 1]$ , for every  $z$ . In particular,  $\mathcal{X}_j^*(-1) = [q_j^l, \tau_j^1]$  and  $\mathcal{X}_j^*(1) = [\tau_j^1, q_j^u]$  for all  $j \in [n]$ . For  $\mu > 1$ ,  $\chi_{\tau_j}(x_j) + \mu x_j$  is strictly increasing, and hence  $\mathcal{X}_j^*(\mu) = \{q_j^u\}$ . Since  $z \leq \mathbf{1}^\top q^u$ ,  $\phi(\mu)$  is affine and non-decreasing over  $(1, +\infty)$ . Similarly, by considering  $\mu < -1$ , we have  $\mathcal{X}_j^*(\mu) = \{q_j^l\}$  and  $\phi(\mu)$  is affine and non-increasing over  $(-\infty, -1)$ . Collecting these facts gives that, for every  $z \in [\mathbf{1}^\top q^l, \mathbf{1}^\top q^u]$ , the dual function  $\phi(\mu)$  is convex and piecewise affine with possible break points at  $\mu = -1$  and  $\mu = 1$ . Therefore,  $g^{\text{out}}(z) = \min_{\mu \in \mathbf{R}} \phi(\mu) = \min\{\phi(-1), \phi(1)\}$ .

As  $\tau_j^1 \in \mathcal{X}_j^*(\mu)$  for  $\mu \in [-1, 1]$ , we have  $\phi(-1) = z - \mathbf{1}^\top \tau^1 + \mathbf{1}^\top \tau^2$  and  $\phi(1) = -z + \mathbf{1}^\top \tau^1 + \mathbf{1}^\top \tau^2$ .  $\phi(-1) \leq \phi(1)$  for  $z \in [\mathbf{1}^\top q^l, \mathbf{1}^\top \tau^1]$ , and  $\phi(1) \leq \phi(-1)$  for  $z \in [\mathbf{1}^\top \tau^1, \mathbf{1}^\top q^u]$ . Therefore,

$$g^{\text{out}}(z) = \begin{cases} z - \mathbf{1}^\top \tau^2 + \mathbf{1}^\top \tau^2 & \mathbf{1}^\top q^l \leq z \leq \mathbf{1}^\top \tau^1 \\ -z + \mathbf{1}^\top \tau^1 + \mathbf{1}^\top \tau^2 & \mathbf{1}^\top \tau^1 \leq z \leq \mathbf{1}^\top q^u \end{cases}$$

Comparing with (15) establishes (i). (ii) follows from the fact that, for a given optimal dual solution  $\mu^*$ ,  $x_j^*(\mu^*) \in \mathcal{X}_j^*(\mu^*)$ ,  $j \in [n]$ , is an optimal primal solution if and only if the constraint  $z = \mathbf{1}^\top x^*$  is satisfied.

### C. Proof of Proposition 3

We first show that the conditions are sufficient. We start by showing that the output functions from  $\Omega\{(g_j^{\text{in}}, X_j)\}_{j \in [n]}$  and  $\Omega\{(g_j^{\text{in}}, \text{conv } X_j)\}_{j \in [n]}$  have the same domain under the given conditions. Since  $\tau_j^1 \in X_j$  for all  $j \in [n]$  and  $\sum_{j=1}^n X_j \cap (-\infty, \tau_j^1]$  is connected,  $\sum_{j=1}^n X_j \cap (-\infty, \tau_j^1] = [\sum_{j=1}^n \min X_j, \sum_{j=1}^n \tau_j^1]$ . Similarly,  $\sum_{j=1}^n X_j \cap [\tau_j^1, \infty) = [\sum_{j=1}^n \tau_j^1, \sum_{j=1}^n \max X_j]$ . Therefore,  $\sum_{j=1}^n X_j = [\sum_{j=1}^n \min X_j, \sum_{j=1}^n \max X_j] = \sum_{j=1}^n \text{conv } X_j$ .

It is straightforward that  $\Omega\{(g_j^{\text{in}}, X_j)\}_{j \in [n]} \leq \Omega\{(g_j^{\text{in}}, \text{conv } X_j)\}_{j \in [n]}$ . Hence it is sufficient to prove the other direction. By Lemma 5,  $\Omega\{(g_j^{\text{in}}, \text{conv } X_j)\}_{j \in [n]}$  is a  $\chi$  function with top point  $\tilde{\tau} := (\sum_{j=1}^n \tau_j^1, \sum_{j=1}^n \tau_j^2)$ . We need to show that  $(\Omega\{(g_j^{\text{in}}, X_j)\}_{j \in [n]})(z) \geq \chi_{\tilde{\tau}}(z)$  for all  $z \in [\sum_{j=1}^n \min X_j, \sum_{j=1}^n \max X_j]$ .

We first consider  $z \in [\sum_{j=1}^n \min X_j, \sum_{j=1}^n \tau_j^1]$ . Let  $X_j$  contain  $m_j$  pieces of intervals. Plus that  $\tau_j^1 \in X_j$  separates an interval of  $X_j$  into two pieces, with possibly one of the two containing the single point  $\tau_j$ , there are  $m_j + 1$  pieces in total. Without loss of generality, label the  $m_j + 1$  intervals  $X_j^k$  in increasing order, that is,  $X_j^k$  such that  $\max X_j^{k-1} \leq \min X_j^k$  for all  $k \in [m_j + 1]$ . In particular, let  $l_j \in [m_j + 1]$  be such that  $\tau_j^1 = \max X_j^{l_j} = \min X_j^{l_j+1}$  for all  $j \in [n]$ . Furthermore, let  $\tilde{\Theta} := \prod_{j=1}^n [m_j + 1]$  and  $\tilde{\Theta}_{\leq \sigma'} := \{\sigma \in \tilde{\Theta} \mid \sigma \leq \sigma'\}$  for all  $\sigma' \in \tilde{\Theta}$ . The notation  $\tilde{\Theta}_{> \sigma'}$  has similar meaning. With these notations,  $X_j \cap (-\infty, \tau_j^1] = \cup_{\sigma_j \leq l_j} X_j^{\sigma_j}$ . Then  $\cup_{\sigma \in \tilde{\Theta}_{\leq l}} \sum_{j=1}^n X_j^{\sigma_j} = \sum_{j=1}^n \cup_{\sigma_j \leq l_j} X_j^{\sigma_j} = \sum_{j=1}^n X_j \cap (-\infty, \tau_j^1] = [\sum_{j=1}^n \min X_j, \sum_{j=1}^n \tau_j^1]$ . It is then sufficient to prove that for all  $\sigma \in \tilde{\Theta}_{\leq l}$ ,  $\Omega(\sigma) = \chi_{\tilde{\tau}}$  over the domain  $\sum_{j=1}^n X_j^{\sigma_j}$ .

Pick arbitrary  $\sigma \in \tilde{\Theta}_{\leq l}$ , without loss of generality, let  $[q_j^l, q_j^u] := X_j^{\sigma_j}$ . Restricted in this domain,  $g_j^{\text{in}}$  is an affine function with slope 1. Lemma 4 implies that  $(q_j^u, q_j^u - \tau_j^1 + \tau_j^2)$  can be treated as the top point of  $g_j^{\text{in}}$  over domain  $[q_j^l, q_j^u]$ . Lemma 5 then implies that  $\Omega(\sigma)$  is an affine function with top point  $(\sum_{j=1}^n q_j^u, \sum_{j=1}^n q_j^u - \sum_{j=1}^n \tau_j^1 + \sum_{j=1}^n \tau_j^2)$ . It is straightforward to check that this top point lies on  $\chi_{\tilde{\tau}}$ . As a result,  $\Omega(\sigma) = \chi_{\tilde{\tau}}$  when evaluated in the domain  $\sum_{j=1}^n X_j^{\sigma_j}$ . By symmetry, the same result can be shown for  $z \in [\sum_{j=1}^n \tau_j^1, \sum_{j=1}^n \max X_j]$ , by considering  $\sigma \in \tilde{\Theta}_{> l}$ .

We now show that the conditions are necessary. Lemma 5 implies that the solution to (14) corresponding to  $(\Omega\{(g_j^{\text{in}}, \text{conv } X_j)\}_{j \in [n]})(z)$  with  $z = \sum_{j=1}^n \tau_j^1$  is unique and  $x_j^* = \tau_j^1$  for all

$j \in [n]$ . In order for  $\Omega\{(g_j^{\text{in}}, X_j)\}_{j \in [n]} = \chi_{\tilde{\tau}}$  to be true, it must be that  $\tau_j^1 \in X_j$  for all  $j \in [n]$ .

We next prove connectedness of  $\sum_{j=1}^n X_j \cap (-\infty, \tau_j^1]$  and  $\sum_{j=1}^n X_j \cap [\tau_j^1, \infty)$ , given that  $\Omega\{(g_j^{\text{in}}, X_j)\}_{j \in [n]} = \chi_{\tilde{\tau}}$ . If we could show  $\max_{\sigma \in \tilde{\Theta}_{\leq l} \cup \tilde{\Theta}_{> l}} \Omega(\sigma) = \chi_{\tilde{\tau}}$ , then the connectedness would follow from the fact that two equal functions must have identical domains. In order to show this equality, it is sufficient to show that for all  $\sigma \in \tilde{\Theta} \setminus (\tilde{\Theta}_{\leq l} \cup \tilde{\Theta}_{> l})$ , either  $\Omega(\sigma) < \chi_{\tilde{\tau}}$  or  $\Omega(\sigma) = \Omega(\sigma')$  for some  $\sigma' \in \tilde{\Theta}_{\leq l} \cup \tilde{\Theta}_{> l}$ . Pick arbitrary  $\sigma \in \tilde{\Theta} \setminus (\tilde{\Theta}_{\leq l} \cup \tilde{\Theta}_{> l})$ , then both  $\{j : \sigma_j \leq l_j\}$  and  $\{j : \sigma_j \geq l_j + 1\}$  are nonempty. Similar to the arguments in previous paragraphs for proving the sufficient condition, let  $[q_j^l, q_j^u] := X_j^{\sigma_j}$ , then Lemma 4 and Lemma 5 imply that  $\Omega(\sigma)$  is a  $\chi$  function with top point  $(\hat{\tau}_1, \hat{\tau}_2)$ , where  $\hat{\tau}_1 := \sum_{\{j: \sigma_j \leq l_j\}} q_j^u + \sum_{\{j: \sigma_j \geq l_j + 1\}} q_j^l$  and  $\hat{\tau}_2 := \sum_{\{j: \sigma_j \leq l_j\}} (q_j^u - \tau_j^1) + \sum_{\{j: \sigma_j \geq l_j + 1\}} (\tau_j^1 - q_j^l) + \sum_{j=1}^n \tau_j^2$  and domain  $[\sum_{j=1}^n q_j^l, \sum_{j=1}^n q_j^u]$ . Simple algebra gives:

$$\chi_{\tilde{\tau}}(\hat{\tau}_1) - \hat{\tau}_2 = 2 \min \left\{ \sum_{\{j: \sigma_j \leq l_j\}} (\tau_j^1 - q_j^u), \sum_{\{j: \sigma_j \geq l_j + 1\}} (q_j^l - \tau_j^1) \right\} \geq 0$$

If both  $\{j : \sigma_j \leq l_j - 1\}$  and  $\{j : \sigma_j \geq l_j + 2\}$  are nonempty, then the above inequality is strict, implying  $(\hat{\tau}_1, \hat{\tau}_2)$  is below  $\chi_{\tilde{\tau}}$  and hence  $\Omega(\sigma) < \chi_{\tilde{\tau}}$ . Otherwise, if either  $\{j : \sigma_j \leq l_j\} = \{j : \sigma_j = l_j\}$  only, or  $\{j : \sigma_j \geq l_j + 1\} = \{j : \sigma_j = l_j + 1\}$  only, or both, then the above inequality becomes equality and  $(\hat{\tau}_1, \hat{\tau}_2)$  lies on  $\chi_{\tilde{\tau}}$ . We consider the first case and show that  $(\Omega(\sigma))(z) < \chi_{\tilde{\tau}}(z)$  for  $z \in [\sum_{j=1}^n q_j^l, \hat{\tau}_1)$  and  $(\Omega(\sigma))(z) = \Omega(\sigma')(z)$  for all  $z \in [\hat{\tau}_1, \sum_{j=1}^n q_j^u]$  and for some  $\sigma' \in \tilde{\Theta}_{\leq l} \cup \tilde{\Theta}_{> l}$ . Similar results are true for the other two cases.

In the case considered,  $q_k^u = \tau_k^1$  for all  $k \in \{j : \sigma_j = l_j\}$ ,  $q_k^l \geq \tau_k^1$  for all  $k \in \{j : \sigma_j \geq l_j + 1\}$ , and the later inequality is strict for at least one  $k$ . Then  $\hat{\tau}_1 > \sum_{j=1}^n \tau_j^1 = \tilde{\tau}_1$ . Combining with Lemma 5, and recalling that  $\hat{\tau}$  lies on  $\chi_{\tilde{\tau}}$ , we get that  $(\Omega(\sigma))(z) < \chi_{\tilde{\tau}}(z)$  for  $z \in [\sum_{j=1}^n q_j^l, \hat{\tau}_1)$  and  $(\Omega(\sigma))(z) = \chi_{\tilde{\tau}}(z)$  for  $z \in [\hat{\tau}_1, \sum_{j=1}^n q_j^u]$ . It remains to show the existence of  $\sigma' \in \tilde{\Theta}_{\leq l} \cup \tilde{\Theta}_{> l}$  such that  $(\Omega(\sigma))(z) = (\Omega(\sigma'))(z)$  for  $z \in [\hat{\tau}_1, \sum_{j=1}^n q_j^u]$ . Such a  $\sigma'$  is constructed as follows:  $\sigma'_k = l_j + 1$  for all  $k \in \{j : \sigma_j = l_j\}$  and  $\sigma'_k = \sigma_k$  for all  $k \in \{j : \sigma_j \geq l_j + 1\}$ . Such a  $\sigma' \in \tilde{\Theta}_{> l}$  ensures that  $\Omega(\sigma')$  and  $\Omega(\sigma)$  have identical top points.

#### D. Proof of Proposition 6

The following lemma, which is also referred to as the geometric version of Farkas Lemma [34], is used below in the proof of Proposition 6.

*Lemma 8* ([19, Sect. 1.4]): Consider a full dimensional polytope  $P \subset \mathbf{R}^d$  with facets  $\Gamma_i^{d-1}$  whose defining hyperplanes are  $H_i := \{x \in \mathbf{R}^d \mid (\pi^i)^\top x = \pi_0^i\}$ , and let  $\Gamma \subset \cap_{i \in S} \Gamma_i^{d-1}$  be a nonempty face of  $P$  for some index set  $S$ . Then,  $\Gamma = \operatorname{argmax}_{x \in P} \mu^\top x$  for some  $\mu \in \mathbf{R}^d$  if and only if there exists  $\theta \in \mathbf{R}_{>0}^S$  such that  $\mu = \sum_{i \in S} \theta_i \pi^i$ .

Let  $\tau(x) := \operatorname{argmax}_{\hat{x} \in P} \{\hat{x}_k \mid \hat{x}_j = x_j, \forall j \neq k\}$  for all  $x \in P$ , and let  $P^t := \cup_{x \in P} \{\tau(x)\}$ . It follows from the definition that every  $x \in P$  is shaded by  $\tau(x) \in P^t$  in direction  $\mathbf{e}_k$ . We now show that  $P^t$  is included in  $\mathbf{e}_k$ -top facets of  $P$ . For each point  $\tilde{x} \in P^t$ ,  $P \cap (\{\tilde{x}\} + (0, +\infty)\mathbf{e}_k) = \emptyset$ , where the set  $\{\tilde{x}\} + (0, +\infty)\mathbf{e}_k$  is the half open ray starting from  $\tilde{x}$  and pointing in the  $\mathbf{e}_k$  direction. The separating hyperplane theorem, e.g., see [35], then implies that there exist  $\mu \in \mathbf{R}^d$  and  $\mu_0 \in \mathbf{R}$  such that  $\mu^\top x \leq \mu_0$  for all  $x \in P$  and  $\mu^\top x > \mu_0$  for all  $x \in \{\tilde{x}\} + (0, +\infty)\mathbf{e}_k$ . The latter implies  $\mu_k = \mu^\top \mathbf{e}_k > 0$ . In order to show that  $\tilde{x}$  is included in a  $\mathbf{e}_k$ -top facet of  $P$ , we consider two cases. First, if  $\tilde{x}$  is in the interior of some facet  $\Gamma_i^{d-1}$ , then, since  $H_i$  is the unique separating hyperplane of  $\Gamma_i^{d-1}$ , we get  $\pi^i = \mu$  and  $\pi_k^i > 0$ . Hence  $\Gamma_i^{d-1}$  is a  $\mathbf{e}_k$ -top facet. Second, if  $\tilde{x}$  is in a lower dimensional face, then consider a non-empty set  $\mathcal{J}$  such that  $\tilde{x} \in \cap_{i \in \mathcal{J}} \Gamma_i$ . By contradiction, from Lemma 8, there exists a  $j \in \mathcal{J}$  such that  $\pi_k^j > 0$ . This implies that  $\tilde{x}$  belongs to the facet  $\Gamma_j^{d-1}$ , a  $\mathbf{e}_k$ -top facet. This establishes (i).

For (ii), pick an arbitrary point  $\hat{x}$  from an arbitrary  $\mathbf{e}_k$ -top facet  $\Gamma_i^{d-1}$ . By definition of a facet,  $\hat{x} \in \operatorname{argmax}_{x \in P} (\pi^i)^\top x$ . This implies that  $\tau(\hat{x}) = \hat{x}$ , i.e.,  $\hat{x} \in P^t$ . It is then straightforward to see that  $\Gamma_i^{d-1}$  remains to be a facet in  $\operatorname{sweep}_k(P)$ , since the hyperplane  $H_i$  contains  $\operatorname{sweep}_k(P)$  on one side.

We now prove (iii). Let  $\Gamma^{d-2}$  be an arbitrary ridge of  $P$  and  $\Gamma_i^{d-1}$  and  $\Gamma_j^{d-1}$  be the two incident facets of  $\Gamma^{d-2}$ . We first prove the conditions to be necessary by considering the following cases:

- (a) if  $\Gamma^{d-2} \subset \bar{H}$ , then  $\operatorname{sweep}_k(\Gamma^{d-2}) = \Gamma^{d-2}$  is of dimension  $(d-2)$  and it is trivial that  $\operatorname{sweep}_k(\Gamma^{d-2})$  is not a facet of  $\operatorname{sweep}_k(P)$ ;
- (b) if neither  $\Gamma_i^{d-1}$  nor  $\Gamma_j^{d-1}$  is a  $\mathbf{e}_k$ -top facet, then all the points in  $\Gamma^{d-2}$  are shaded by some other points in  $P$  and hence  $\operatorname{sweep}_k(\Gamma^{d-2})$  is not a facet of  $\operatorname{sweep}_k(P)$ ;
- (c) if both  $\Gamma_i^{d-1}$  and  $\Gamma_j^{d-1}$  are  $\mathbf{e}_k$ -top facets, then (ii) of the proposition implies that both  $\Gamma_i^{d-1}$  and  $\Gamma_j^{d-1}$  remains to be facets of  $\operatorname{sweep}_k(P)$ . Since a ridge is contained in exactly two facets [20, Chapter 3],  $\operatorname{sweep}_k(\Gamma^{d-2})$  can not be a facet of  $\operatorname{sweep}_k(P)$ .

We now prove the sufficient condition. Let  $\Gamma^{d-2} \notin \bar{H}$  be a boundary ridge and, without loss of generality, let the incident facets be such that  $\Gamma_i^{d-1}$  is a  $\mathbf{e}_k$ -top facet and  $\Gamma_j^{d-1}$  is either a  $\mathbf{e}_k$ -facet or a  $\mathbf{e}_k$ -bottom facet, i.e.,  $\pi_k^i > 0$  and  $\pi_k^j \leq 0$ . Proposition 5 implies that  $\operatorname{sweep}_k(\Gamma^{d-2})$

is of dimension  $(d - 1)$ . Therefore,  $\text{sweep}_k(\Gamma^{d-2})$  is a facet if it is a face of  $\text{sweep}_k(P)$ . We now construct the defining hyperplane  $H$  of  $\text{sweep}_k(\Gamma^{d-2})$ . Let  $\theta := \pi_k^i / (\pi_k^i - \pi_k^j) \in (0, 1]$ ,  $\pi := (1 - \theta)\pi^i + \theta\pi^j$  and  $\pi_0 := (1 - \theta)\pi_0^i + \theta\pi_0^j$ . It is straightforward that  $\pi_k = 0$ . Define  $H := \{x \in \mathbf{R}^d \mid \pi^\top x = \pi_0\}$ . It is sufficient to show that  $\text{sweep}_k(\Gamma^{d-2}) \subset H$  and  $H$  contains  $\text{sweep}_k(P)$  on one side. Since  $\pi_k = 0$ ,  $\text{sweep}_k(\Gamma^{d-2}) \subset H$  if and only if  $\Gamma^{d-2} \subset H$ . The latter is straightforward from the definition of  $H$ . In order to show that  $H$  contains  $\text{sweep}_k(P)$  on one side, we separately consider the two possibilities for  $\pi_k^j$ . If  $\pi_k^j < 0$ , and hence  $\theta \in (0, 1)$ , then Lemma 8 implies the claim. If  $\pi_k^j = 0$ , and hence  $\theta = 1$ , then  $H = H_j$ , the defining hyperplane of  $\Gamma_j^{d-1}$ . This implies the claim trivially.